FH Aachen

Masterarbeit

IDENTIFICATION OF AFFECT PATTERNS FROM BIOSIGNALS

Jossin Antony

2014

FH AACHEN
UNIVERSITY OF APPLIED SCIENCES

FH Aachen

Fachbereich Maschinenbau und Mechatronik

Studiengang Mechatronik

Masterarbeit

IDENTIFICATION OF AFFECT PATTERNS FROM BIOSIGNALS

vorgelegt von **Jossin Antony**

Matrikel-Nr. **413030**

Referent: Prof. Dr.-Ing. Stephan Kallweit

Korreferent: Prof. Dr. rer. nat. Alexander Ferrein

Externer Betreuer: Karan Sharma, MSc.

Datum: 28.04.2014

In Zusammenarbeit mit: Deutsches Zentrum für Luft- und Raumfahrt e. V. (DLR)

vertraulich bis: 01.05.2020

Erklärung

Ich versichere hiermit, dass ich die vorliegende Arbeit selbständig verfasst und keine anderen als die im Quellenverzeichnis angegebenen Quellen benutzt habe. Stellen, die wörtlich oder sinngemäß aus veröffentlichten oder noch nicht veröffentlichten Quellen entnommen sind, sind als solche kenntlich gemacht. Die Zeichnungen oder Abbildungen in dieser Arbeit sind von mir selbst erstellt worden oder mit einem entsprechenden Quellennachweis versehen. Diese Arbeit ist in gleicher oder ähnlicher Form noch bei keiner anderen Prüfungsbehörde eingereicht worden.

Aachen, April 2014

Acknowledgements

My deepest gratitude goes to my supervisor at DLR, Karan Sharma who was a constant source of inspiration to me. His expert guidance and support instilled in me the motivation to pursue research in its entire rigor.

I would like to extend my sincere thanks to my second supervisor Dr. Claudio Castellini for showing me the beauty of Machine Learning techniques. His simplistic yet powerful approach to problem solving introduced to me new horizons in this exciting field of engineering.

I would like to thank Prof. Dr.-Ing. Stephan Kallweit and Prof. Dr. rer. nat. Alexander Ferrein, my supervisors at the Fachhochschule Aachen for their valuable guidance and immense support throughout the period of my thesis.

My sincere gratitude is extended to Dr. Egon L. van den Broek for his timely support and advise in every phase of my thesis.

I would like to thank our project head at DLR, Dipl.-Ing. Johann Heindl for his support and guidance.

Sincere thanks are extended to Miguel Neves for being there and keeping me straight during difficult times.

Thanks are also due to all of my friends and colleagues at the DLR- you were always there for me, you were the test subjects in my experiments and without you people none of my research dreams would have been realized.

Finally it goes without saying, my deepest love and gratitude to my family for all the support and wishes.

Jossin Antony

Abstract

In her seminal work, Rosalind Picard defined *Affective Computing as, computing that relates to, arises from, or deliberately influences emotions.* The aim of the thesis is to explore the possibility of application of affective computing concepts to the DLR Robotic Motion Simulator (DLR-RMS). The DLR-RMS is a serial kinematics based platform that uses an industrial robot to provide the motion cues to an attached simulation cell. By making the DLR-RMS 'emotion aware', the simulator can e.g., adapt simulations to the subjective needs of its users. This thesis is one of the first steps taken towards fulfilling the aforementioned goal and therefore, concerns itself primarily with laying the ground work for further studies. To do the same, a ground based (not on the simulator) experiment that uses video clips as stimuli (instead of video and motion, as on the simulator) was designed and undertaken to acquire the emotional/affective response from 30 human subjects. A novel user feedback interface, which employs a joystick to acquire subjective evaluation for video clips, was also developed. This interface allows the subject to continuously state his/her emotional status that was elicited by viewing the video clips. The data acquired during the experiments was analysed using statistical techniques e.g., Principal Component Analysis (PCA) to determine the trend in the recorded data. The thesis concludes by presenting the results of the data analysis, which show favourable and expected patterns in data that validate the design and methodology of the experiment and lay the ground work for further experiments to be undertaken on the DLR-RMS.

Contents

I Introduction **15**

1 Introduction **17**

1.1 Motion Simulator: Overview 17

1.2 The Modern Motion Simulator 17

1.3 The DLR Robotic Motion Simulator 18

1.4 Motivation 19

2 Task Definition **23**

2.1 Thesis Objectives 23

2.2 Organisation of the Thesis 23

3 Affect Computing-Introduction **25**

3.1 Defining Emotion and Affect 25

3.1.1 Affective Experiences of Arousal and Pleasure 25

3.1.2 Specificity of Physiological Parameters to Arousing Conditions 26

3.2 Affect Computing - State of the Art 27

3.2.1 Affect Computing-Concepts 27

3.2.2 Affect Computing-Related Research 28

4 Physiological Signals **31**

4.1 The Physiological Features 31

4.1.1 Cardiac Activity 31

4.1.2 Skin Conductance /Electrodermal Activity 34

4.1.3 Respiration 35

4.1.4 Electromyographic (EMG) Activity 36

4.1.5 Temperature 37

II Design of the Experiment **39**

5 Affect State Estimation from Video Stimuli **41**

5.1 Introduction 41

5.2 Aim 41

5.3 Structure of the Experiment 43

6 Video Segments as Stimuli **45**

6.1 Video segments as stimuli 45

6.2 The Film-Stimuli Set 45

6.3 The Labelling System 46

6.4 The Labelling UI 47

6.5 Data Acquisition - System and Procedure 49

6.5.1 Instrumentation 49

6.6 Data Acquisition Program 50

6.6.1 State 1-Initialize 51

6.6.2 State 2-Start 51

6.6.3 State 3-Data Acquisition 51

6.6.4 State 4-Stop and Release 52

7 Experiment procedure **55**

7.1 Participants 55

7.2 Environment 55

7.3 Sensors 55

7.3.1 **T**he ECG sensor 55

7.3.2 **T**he BVP sensor 56

7.3.3 **T**he Electrodermal Activity (EDA) sensor 57

7.3.4 **T**he Respiration sensor 58

7.3.5 **T**he Temperature sensor 58

7.3.6 **T**he EMG sensor 59

7.4 Procedure 60

III Data Analysis **63**

8 Feature Extraction **65**

8.1 Biosignals-Feature Extraction 65

8.1.1 ECG Feature Extraction 65

8.1.2 BVP Feature Extraction 68
8.1.3 Electrodermal Activity Feature Extraction 69
8.1.4 Respiration Feature Extraction 70
8.1.5 EMG Feature Extraction 71
8.1.6 Data from Labelling System 71

9 Data Analysis and Results **75**
9.1 Feature Space 75
9.2 Features vs. Video Segments 76
9.3 Pattern Identification and Visualization 79
9.3.1 Formulation of PCA 79
9.3.2 Data Visualisation 80
9.4 Conclusion and Future work 81

A System Usability Scale (SUS) Survey **83**

Part I

Introduction

Chapter 1

Introduction

1.1 Motion Simulator: Overview

A motion simulator is 'used for simulating the working characteristics of motion vehicles'[1]. A modern motion simulator uses a synchronized combination of motion, visual and audio cues to transfer the sensation of a realistic motion to the human passenger in the simulator. The overall aim of the motion simulation system is to give a feeling of immersion into the environment being simulated.

Motion simulators are used in different fields of engineering, research and entertainment:

1. In the aviation industry, motion simulators are primarily used as flight simulators to train pilots e.g., The Airbus Full Flight Simulator [2].They also find application in related researches such as pre-production examination of pilot ergonomics, assessment of crew behavior under various stressors etc [3].

2. In the automotive industry motion simulators are used as driving simulators. They are used in research to evaluate the safety of the car, driver behaviour [4], the human-machine interface (HMI) design [5] etc.

3. Motion simulators have also found application in the gaming and entertainment industry. In the entertainment industry motion simulators are used to provide theme-centered fun rides.[6].

4. Motion simulators are also used as virtual racing simulators in the gaming industry [7] [8].

1.2 The Modern Motion Simulator

Modern motion simulators are complex mechatronic systems, in which a simulator cabin is mounted on a motion platform and audio, visual, motion and tactile cues are implemented in

such a way so as to provide the illusion of being in a real vehicle.[9].

A modern high-end motion simulator based on the Stewart Platform is illustrated in the figure [10]:

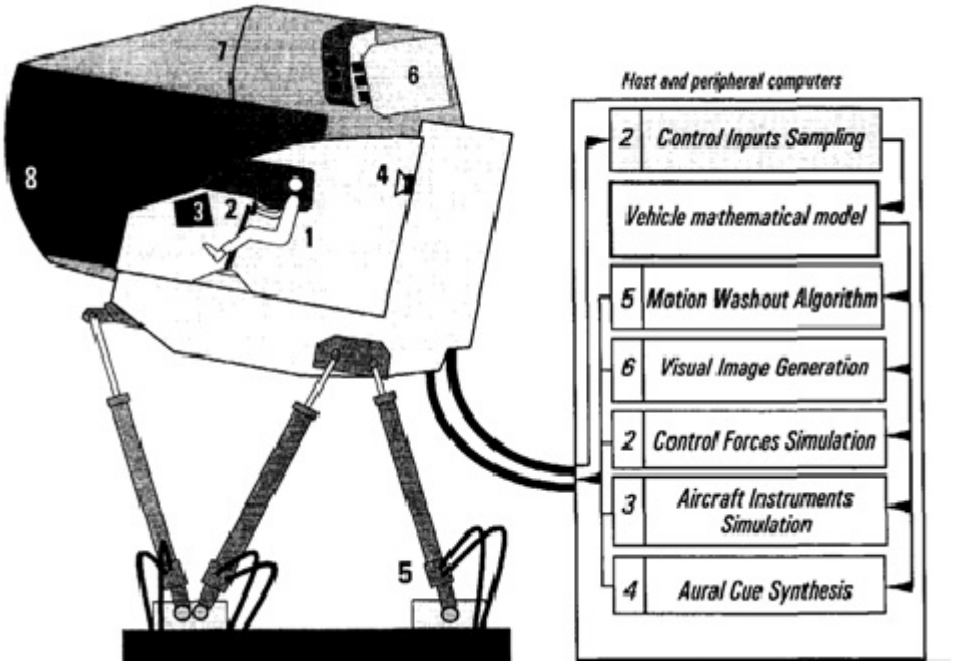

Figure 1.2.1: Modern motion-flight simulator based on Stewart Platform (source:[10])

Schematic of a modern motion (flight) Simulator: The pilot (1) manipulates the controls (2), which are sampled. The scaled control signals are applied to the mathematical model of the vehicle. The resulting accelerations are passed through the motion washout algorithm to generate command signals to the motion-base (5). Simulated aircraft position and orientation command the visual image generation, which presents the image through the projectors (6), and rear-projection screen (7) which is viewed by the pilot via a spherical mirror(8). Aircraft instrument responses (3) are computed, and the aural cues are synthesized and reproduced by the audio system (4) [10].

1.3 The DLR Robotic Motion Simulator

The fundamental design concept of almost every high-end motion simulator till date is based on parallel kinematics commonly known as 'Stewart-Platform' (aka Stewart-Gough Platform)[11]. Besides offering many advantages [12] stewart platform have some inherent disadvantages which arise mainly from the parallel configuration of the kinematic axes. They are expensive to deploy and offer a limited range of motion [13]. To surpass these limitations the researchers at the German Aerospace Centre (DLR) have developed a motion simulation platform based on serial

kinematics [14] [15].

The DLR Robotic Motion Simulator (DLR-RMS) 'is a serial kinematics based platform that employs an industrial robot to impart motion cues to the attached simulator cell' [13]. The latest version of the DLR-RMS installed at the DLR-Robotics and Mechatronics centre (DLR-RMC) is based on a KUKA KR500 industrial robot with 6 degrees of freedom (6 DoF), mounted on a KUKA KL3000 linear axis of length of 10m. It can be used for various online as well as offline simulations.

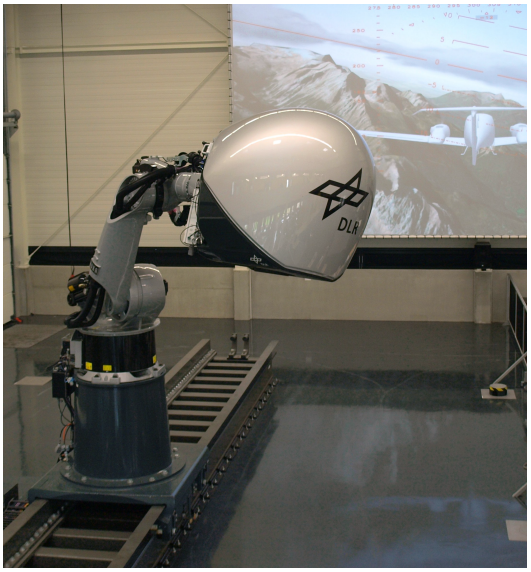

Figure 1.3.1: The DLR Robotic Motion Simulator (DLR-RMS)

The distinctive advantages of the DLR-RMS over the traditional motion simulators based on Stewart platform are the lower costs, increased workspace and maneuverability, including the ability to perform rolls or loops [16].

1.4 Motivation

From section 1.2 it was seen that the aim of the motion simulation platform is to provide a virtual immersive environment to the user. A modern motion simulator should 'look, sound, feel and act like the real vehicle which it simulates' [3]. The dimension of 'feeling' gains more importance in simulator experience. This implies that the simulation experience should be evaluated from the user-point of view (Fig.1.4.1). Another aspect of this approach is the safety of the user. The user being at the center of the simulation, his safety is of paramount importance. Research at the DLR on user safety ([17],[13]) has shown that the DLR-RMS cannot inflict life threatening injuries on the user. A natural continuation of this research is the investigation into the concept of user experience.

A user's experience in the simulator is influenced by several different aspects of simulation,

which can range from the ergonomics of the cell to the quality and preciseness of the A/V and motion cues. Issues with ergonomics (e.g., the seating setup) and cueing are expected to generally influence all users in almost the same manner i.e., a bad seating setup will probably be bad for majority of the users. On the other hand, the user's perceptual experience can be very subjective e.g., one user may find a simulation 'thrilling/entertaining', while another might find it scary. In essence, this means that users might exhibit different emotional responses to a simulation. Thus it becomes imperative that the user perceptual experience or 'feeling' is evaluated. This evaluation should be based on a measurable, comprehensive assessment of the expressed emotional state (or affect state, explained in detail in subsequent sections) of the user throughout the simulation time.

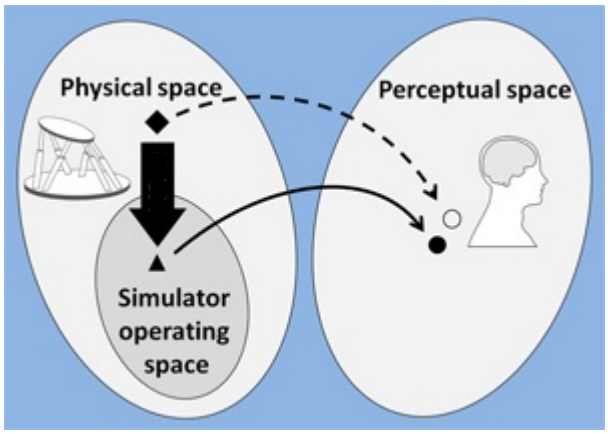

Figure 1.4.1: Simulator perception space
(source:[18])

The importance of the assessment of the user 'affect-state' in motion simulation platforms especially in the context of the DLR-RMS, is discussed below:

1. Offline simulation scenarios- In offline simulation scenarios of the DLR-RMS, the affect-state estimation of the user can be used to increase the overall fun-factor of the ride.

   To elaborate, during an offline simulation of the DLR-RMS, e.g., a fun-ride in an amusement park, the simulator is programmed to provide a thrilling experience to the human passenger. For the same, the manipulator undertakes 'exciting' motions involving high accelerations and velocities. This then leads to the question: When does the user, immersed in a simulation, get from the pleasant phase of excitement to less desired situations such as panic? Is there a way to estimate the 'emotional-state' of the user during the simulator ride? From the results thus obtained, is it possible to evaluate the ride-quality as 'exciting', 'scary', 'boring' etc.? This becomes particularly important in the case of the DLR-RMS, because the DLR-RMS is a viable commercial product. Early prototypes have already been commissioned in amusement parks to provide thrill rides to people.[6] The

potential passengers on the simulator comprise of people belonging to different comfort zones of accelerations and movements and the affect state analysis ensures not only a safe and exciting ride, but also a highly customizable ride experience.

2. Online simulation scenarios - The results obtained from the offline simulation scenarios can be extended to online simulation scenarios as well. For example, in pilot training using simulators, mental workload assessment of pilots and fatigue in aviation studies play a crucial role [19] [20]. The affect state studies can very well be used to assess the pilot cognitive activity, task-related stress, attention and vigilance etc [21] [22] [23]. The affect state studies can also be used to study and improve the fidelity of the simulator in terms of perception. Bowles and Pope proposes that, *there is a need for methodologies to measure pilot perceptual experience in assessing simulator subsystem fidelity...By providing an index of the congruence of the pilot's expectation, based on his internal model of the real world, with the cues actually presented in the simulator, the characteristic of the ER would contribute in a very specific way to the assessment of simulator realism* [21].[1]

3. Medical applications - Affect state studies in simulation scenarios can also provide valuable information in treating aviophobia (fear of flying) using virtual reality exposure [24] [25].

[1] ER is evoked response, extracted from ongoing electrical activity of the brain obtained from the electroencephalograph (EEG), proposed by Bowles and Pope. It is analogous to the affect state determination proposed by us. We propose that affect state determination may provide more insight into this problem than the EEG dependent ER.

Chapter 2

Task Definition

2.1 Thesis Objectives

In the previous chapter the motivation for affect state estimation in motion simulators was presented. The aim of this thesis is to develop a framework that lays the grounwork for application of Affective computing concepts on the DLR-RMS. The main objectives are as follows:

1. Provide a theoretical base for the application of affective computing concepts on the DLR-RMS.

2. Design an experimental setup (on ground, using video stimuli) to validate the proposed hypotheses from step 1. This includes:

   - Identification of suitable sensory input parameters.
   - Procurement of sensors, data acquisition devices and their integration into the test set-up.
   - Conception, development and validation of a joystick interface for subjective affect evaluation of dynamic stimuli.

3. Validating the set-up by undertaking experiments (user study) for affect state estimation from video stimuli.

4. Data analysis, verification and validation of the results.

2.2 Organisation of the Thesis

The thesis is organized in 3 parts:

In part I the premises of the problem, the motivation and the aim of the thesis are introduced. The basic concepts of 'affect' and 'affect-state estimation' are also discussed and an exhaustive

literature review on the state of the art of the field including a study on the relevant sensory input features is presented.

In part II the design and setup of the experimental procedure for affect state estimation from video-stimuli is elaborated. The selection of the stimuli, the development of the labelling interface, the data acquisition set up and the methodology of the experiment are presented.

In part III the data analysis procedure and the verification and validation of the derived results are discussed.

Chapter 3

Affect Computing-Introduction

3.1 Defining Emotion and Affect

In this chapter the terms 'emotion' and 'affective state' are defined in the context of the present research. There has been never a consensus on the definition of 'emotion'and a number of theories exist [26]. For this research work the following definition of emotion by Kleinginna and Kleinginna [27] is accepted as a standard definition:

Emotion is a complex set of interactions among subjective and objective factors, mediated by neural/hormonal systems, which can

1. *give rise to affective experiences such as feelings of arousal and pleasure / displeasure;*
2. *generate cognitive processes such as emotionally relevant perceptual effects, appraisals, labeling processes;*
3. *activate widespread physiological adjustments to the arousing conditions; and*
4. *lead to behavior that is often, but not always, expressive, goal directed, and adaptive.*

This definition directs to the following modalities of emotions relevant in the present context:

3.1.1 Affective Experiences of Arousal and Pleasure

Russell defined Affect as *'neurophysiological state that is consciously accessible as a simple, non-reflective feeling that is an integral blend of hedonic (pleasure-displeasure) and arousal (sleepy-activated) values'*[28]. Furthermore, according to Russell, it is similar to what Thayer called 'activation' [29], what Watson and Tellegen called 'affect' [30], what Morris called 'mood' [31], and what is commonly called a 'feeling'. At a given moment, the conscious experience or the raw feeling is a single integral blend of two dimensions, as shown in the figure 3.1.1. The horizontal dimension marks the pleasure-displeasure. Some authors use the term 'valence' to describe this

effect [32]. This feeling is an assessment of one's current condition and ranges from one extreme (e.g., distress/sad) through a neutral point to its opposite extreme (e.g., elated/happy). The vertical dimension, arousal, is one's sense of mobilization and energy. It ranges from sleep-/drowsiness, through various stages of alertness to frenetic excitement. According to Lang, *all emotions can be located in the two-dimensional space, as coordinates of Affective valence and arousal* [32].

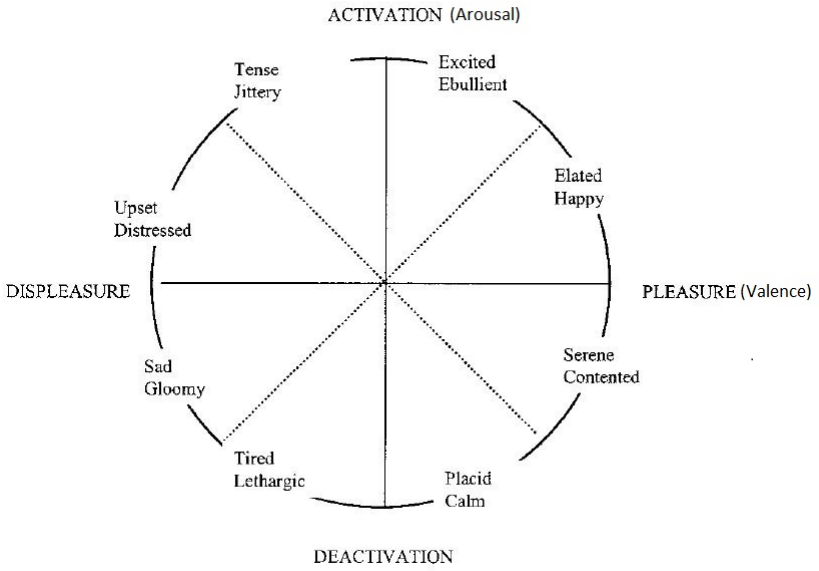

Figure 3.1.1: Valence-Arousal model of emotion
(source:[28])

3.1.2 Specificity of Physiological Parameters to Arousing Conditions

Physiological arousal always accompanies an emotional episode *facial, vocal, and autonomic changes occur and are accounted for (a) by core affect and (b) as part of, preparation for, or recovery from instrumental action* [28].These autonomic changes in the body are expressed as physiological arousals. The prime instigators initiating these changes in the human body are the Amygdalae, located in the temporal lobes of the brain [32] and continued and maintained by the autonomic nervous system (ANS), part of the peripheral nervous system. The autonomous nervous system (ANS) consist of the sympathetic nervous system (SNS) and the parasympathetic branch (PNS).

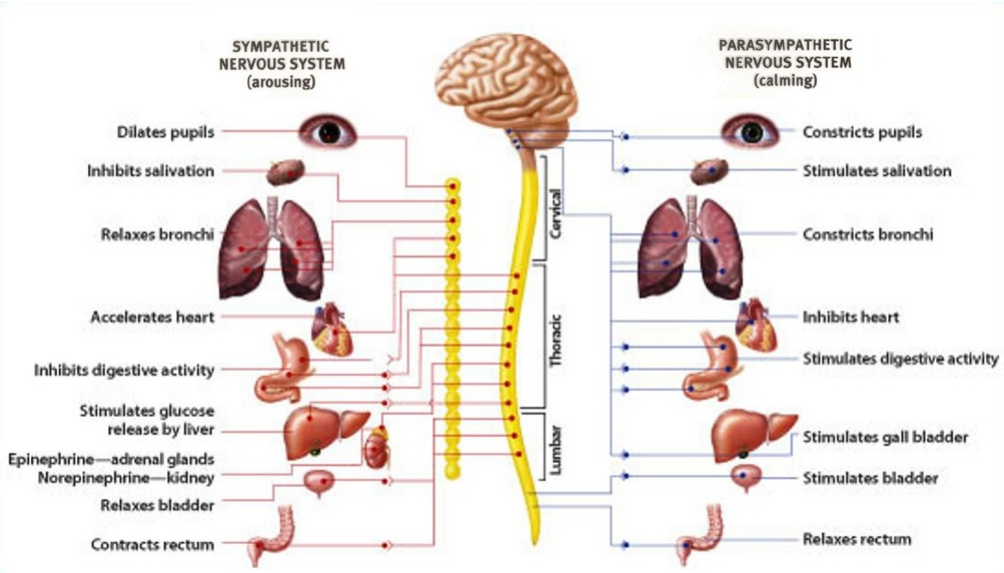

Figure 3.1.2: Functions of ANS

(source:[33])

The SNS primes the body in a perceived emergency situation by increasing the overall activities of muscles, heart, pupil dilation, respiration, adrenal activity etc.('fight or flight' functions). The PNS, on the other hand, function in contrast to the SNS branch and is associated with more vegetative functions such as digestion, relaxation, sexual activity etc.('Rest and digest functions')[34]. Under normal situations there is a balance between these two systems placing the body in a state of homeostasis. However under a state of mental stress this balance will be altered[35]. Kreibig [36] has reported considerable ANS response specificity in emotion from a review of 134 publications that studied emotional effects on peripheral physiological responding in individuals. The physiological parameters studied included the variations in cardio-vascular activity, electrodermal activity, and respiratory activity. Collet et al. [37] also provide evidence to demonstrate the specificity of patterns in autonomic reactions to emotional stimuli. Six ANS parameters were recorded during their experiments: skin conductance, skin potential, skin resistance, skin blood flow, skin temperature and instantaneous respiratory frequency. Evidences for emotion-specific patterns in autonomous nervous activity were also reported by Ekman, Levenson and Friesen [38].

3.2 Affect Computing - State of the Art

3.2.1 Affect Computing-Concepts

In the section 3.1.2 it was seen that much literary evidence exist to establish the correlation of physiological parameters with the exuded emotions. This, in turn, suggests a way of estimating

the affect state or state of emotion of an individual solely from the measurement of his/her physiological parameters. The possibility was explored as early as 1995 by R.W Picard, and described by the term 'Affective computing', and since then has been supplemented by various researches in the field.

'Affective computing' is defined by Picard as, *computing that relates to, arises from, or influences emotions*[39]. Picard further proposes that the recognition of emotion states may be achieved by combining various physiological responses which vary with time and measured through affective wearable computers. The physiological responses include heart rate, systolic and diastolic blood pressure, pulse, pupillary dilation, respiration, skin conductance and temperature. These measurements lead to successful recognition during voluntary as well as involuntary expression of emotion. Affect recognition is more accurate, when it combines multiple kinds of signals from the user with information about the user's context, situation, goals and preferences[40].

3.2.2 Affect Computing-Related Research

In this section a brief overview of research pertaining to affective computing is presented:

1. In 2000, Healey validated the hypotheses put forward by Picard in three types of settings [41]:

   (a) A highly constrained laboratory setting- The tests were designed to identify unique physiological patterns, when the test subject intentionally expressed eight emotions: anger, hate, grief, platonic love, romantic love, joy, reverence and no emotion. The physiological parameters measured included the Cardiac activity, Electrodermal activity (EDA), Electromyographic activity (EMG) and Respiration. The physiological features measured exhibited a success rate of 81 % for discriminating the eight emotions.

   (b) An unconstrained ambulatory environment- Affective wearable computers measured the physiological parameters of test subjects who went on with their daily activities. In this setting the motion artefacts overwhelmed the affective signals, and emphasized the need for more novel systems for accurate affect state determination.

   (c) A more constrained automotive environment- The physiological stress involved in the physical task of driving was recorded using affective sensors. A recognition rate of 96 % for detecting driver stress was achieved.

2. Rani et al. have studied the possibility of integrating robots with affect detecting systems for better Human Computer Interaction (HCI), largely based on affect state recognition

of humans by computer systems. The figure illustrates the framework proposed by Rani et al.[42].

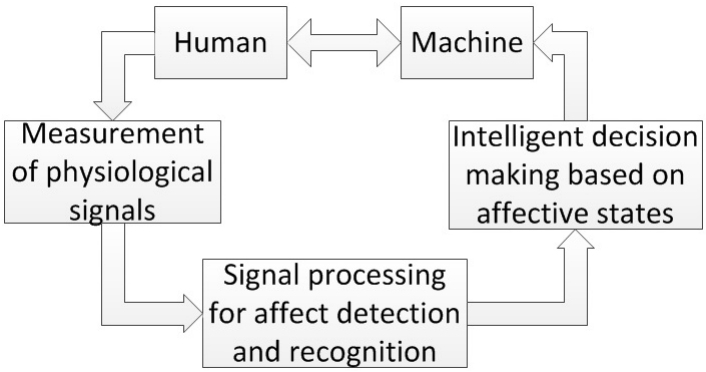

Figure 3.2.1: Human-machine interface based on affect states, proposed by Rani et al. (source:[42])

The physiological signals of the person interacting/ cooperating with the machine are recorded. The probable affect state of the person is estimated from the physiological signals using pattern identification tools. The machine then decides the subsequent course of actions based on the affective state information along with other environmental inputs[42][43]. The focus in her work was on identifying one particular affect state - Anxiety[3]. In later experiments Rani et al. successfully demonstrated an implicit communication between a human and robot wherein the robot detects and recognizes anxiety in its human operator and modifies its task sequence to accommodate a suitable response.[35] A comparative study of the most popular machine learning techniques applied to the domain of affect detection - K-Nearest Neighbour, Regression Tree (RT), Bayesian Network and Support Vector Machine (SVMs) was also conducted. The results showed that SVMs gave the best classification accuracy.[45].

3. Kulic and Croft estimated human affect state in real time, using robot motions as stimuli and physiological signals such as the heart rate, electrodermal activity and facial muscle contractions as inputs to the system [46]. They developed a Hidden Markov model (HMM) based affect state classifier for estimating arousal and valence.

4. Katsis et al. evaluated emotional states in car-racing drivers. The physiological parameters assessed included facial electromyograms, electrocardiogram, respiration and electrodermal activity. They identified specific emotional classes - high stress, low stress, disappointment and euphoria from data obtained in simulated racing conditions. SVMs

[3]Anxiety- something felt, an emotional state that includes feelings of apprehension, tension, nervousness, and worry accompanied by physiological arousal, as defined by Freud [44].

and adaptive neuro-fuzzy inference system (ANFIS) were used for classification and an overall classification rate of 79.3 % was achieved for the SVM and 76.7 % for the ANFIS [47].

5. Liu et al. proposed a human-robot interaction framework for autism rehabilitation based on affect recognition. The affective states studied were pleasure, anxiety, and engagement that were relevant in autism rehabilitation. The affect state classifier was based on support vector machines (SVM) and yielded reliable prediction with approximately 83 % success [48].

6. Researches on similar lines were also conducted by Kim et al. [49], Hudlicka and Mcneese [50], Zhai and Barretto [51], Scheirer et al. [52], prendinger et al. [53],Lisetti and Nasoz [54], Van den Broek[55] etc.

It has been shown in this chapter that conclusive evidence in literature exist to validate the application of affect computing in various scenarios. The successful deployment of an affect estimation system is highly dependent on the selection of the input parameters as well. The input parameters in affect computing are the physiological signals. The various physiological signals significant in the context of affect state estimation are presented in the next chapter.

Chapter 4

Physiological Signals

Affect estimation in humans can be achieved from a large range of features that are of different nature[56]:

- Visual features - facial expressions, body gestures etc.
- Audio features - pitch, energy, frequency etc. of speech
- Physiological features- heart rate, skin conductivity, brain and scalp signals (EEG) etc.

Of these, certain psycho-physiological signals (or Biosignals) are prefered as inputs in affect computing because [26]:

1. These signals are hard to be manipulated or masked unlike the video or audio features, which can be manipulated to some extent.
2. The biosignals offer continuous signals as opposed to speech or facial expressions which are not always overt.

4.1 The Physiological Features

4.1.1 Cardiac Activity

Cardiac activity is one the most studied physiological features in emotion estimation. Levenson et al.[57] reported changes in heart rate as indicator of fear and anger. Roscoe[19] studied heart rate as indicator of stress and mental workload in real and simulated aviation scenarios. Mulder et al.[58] reported increased heart rate and decreased heart rate variability during effortful mental processing. Hudlicka and Mcneese [50] argue that the best practical signal for arousal detection is the heart rate. Kreibig, in her review of 134 publications on 'Autonomic nervous activity in emotion' [36] reported increased cardiac activity in several high arousal situations like fear, anger etc.

4.1.1.1 Electrocardiogram (ECG)

An electrocardiogram is a graphic tracing of the variations in electrical potential caused by the excitation of the heart muscle, detected at the body surface and is used to measure the cardiac activity[59].

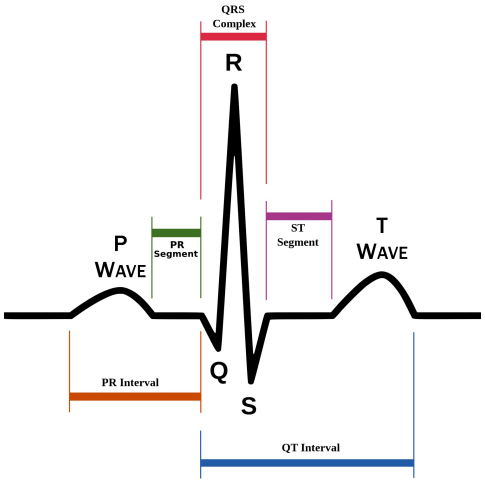

Figure 4.1.1: Schematic diagram of normal sinus rhythm for human heart

The important features derived from the ECG are the heart rate (HR) and the heart rate variability (HRV). Hear rate is the number of heart beats in a minute and is typically 70-80 beats per minute at rest [35]. Heart rate is derived from the inter beat interval, which is the time interval between 2 consecutive QRS complexes[35](Fig.4.1.1). The heart-rate variability (HRV) is defined as the quantitated fluctuations in the heart rate[60]. HRV is measured in both time and frequency domains. The time series measurement of HRV include statistical methods like the variance and the mean absolute deviation of the interbeat inbtervals[26]. In the frequency domain HRV measures the sympathetic and parasympathetic influences on heart rate and can yield information about the emotional reactions[61]. A power spectral density analysis on the inter beat interval data reveals 2 distinct regions; a low frequency region between 0.04 and 0.15 Hz and a high frequency region between 0.15 and 0.40 Hz. The low frequency regions indicate the sympathetic nervous influence and the high frequency region is associated with the parasympathetic nervous activity[35] (Fig.4.1.2).

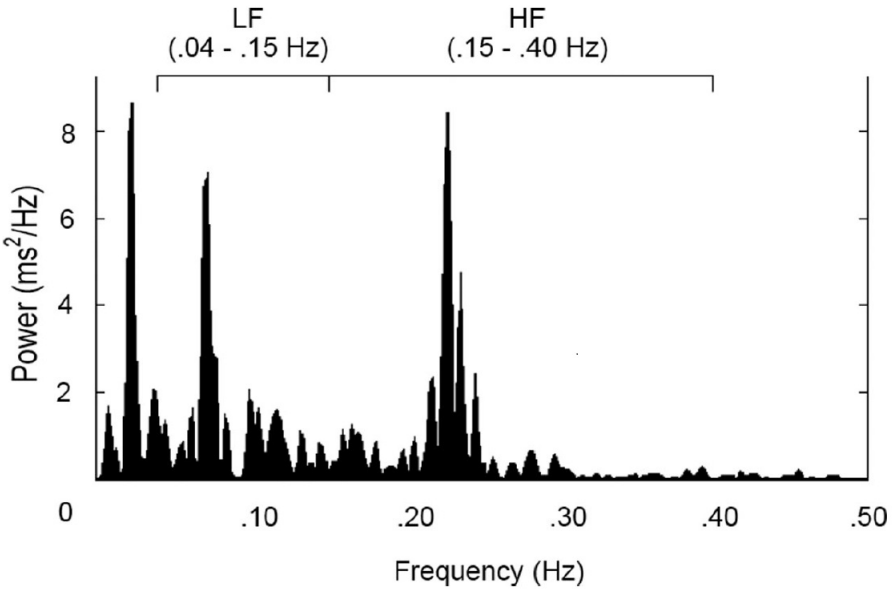

Figure 4.1.2: An example of a heart rate variability power spectrum (Source:[61]).

The low-frequency (LF) component occurs between .04 and .15 Hz and the high-frequency (HF component occurs between .15 and .40 Hz.

4.1.1.2 Blood Volume Pulse (BVP)

The heart rate parameters are also measured using a photoplethysmograph commonly known as a Blood volume pulse (BVP) sensor. The BVP sensor is fitted over a finger or earlobe and emits infra-red light into the tissue. The amount of back-scattered light is dependent on the blood flow through the blood vessels. This varying light is captured by a sensor to produce a pulse waveform[62].

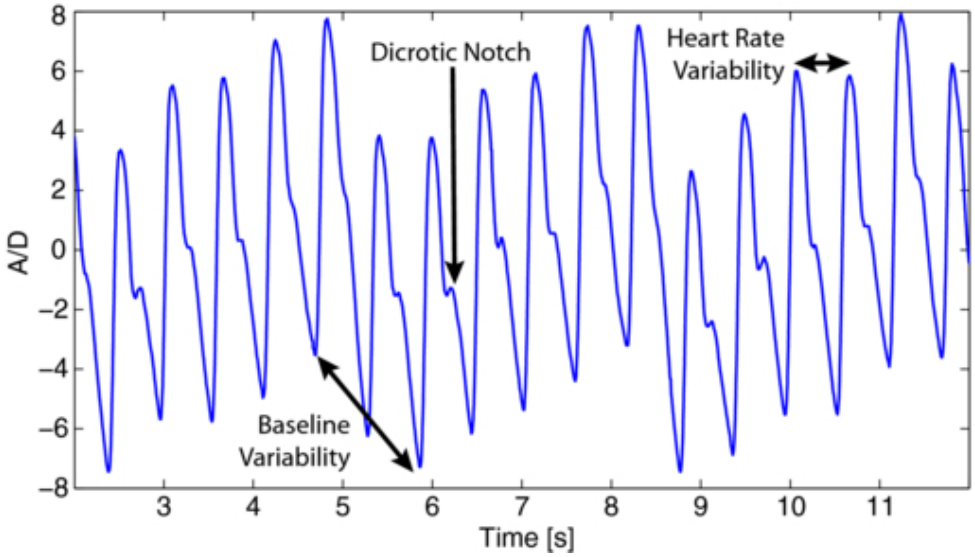

Figure 4.1.3: The BVP signal (source:[63])

The BVP pulse is synchronous with the beating of the heart and is therefore a source of heart rate [64]. The BVP sensor is very easy to place and operate, requiring no site preparation and electrodes, but has the drawback of being prone to motion artifacts[41].

4.1.2 Skin Conductance /Electrodermal Activity

Electrodermal activity (EDA) (also known as 'skin conductance') is a general term for the electrical activity originating from eccrine sweat glands and their associated dermal and epidermal tissues[65]. In the context of emotion studies, the phenomenon of skin conductance gains importance because the eccrine sweat glands are innervated by nerve fibers of the sympathetic system and the measured electrodermal indices reflect psychological responses to stimuli[65].

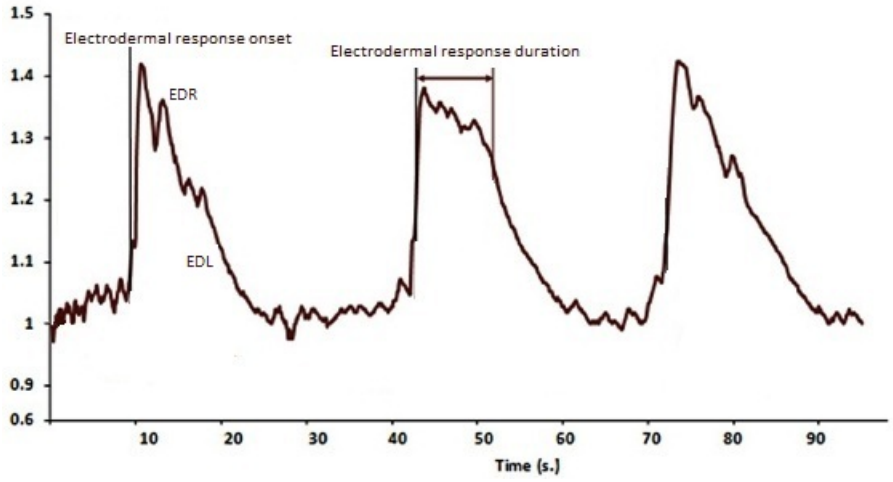

Figure 4.1.4: The typical EDA signal
(source:[66]).The fast changing EDR is superimposed on the relatively slow changing EDL.

The electrodermal signal is constituted by two different (and quasi-independent) components (Fig.4.1.4):

1. The slow changing component known as the *'tonic component'* or Electrodermal level (EDL).

2. A fast changing component called the *'phasic component'* or Electrodermal response (EDR).

The *tonic component* is related to the general arousal level of the individual and the *phasic component* signifies the fast response to a stimuli[67]. EDA response studies gain special attention in the context of 'anxiety studies'. According to Dawson et al.[68], the EDA system is influenced by *'the activation of a neurophysiological behavioral inhibition system that is involved in responding to punishment, to passive avoidance, or to frustrative no reward.'* Thus it represents an 'Anxiety system' and the EDA response should be the first choice of study if the

investigator is interested in the reactions of the subject to a situation that elicit unavoidable anxious state[68]. It should be noted that the EDR is sensitive to a various stimuli characteristics like the stimulus intensity, emotional content significance etc. Therefore an accurate psychological interpretation of the EDR involves knowledge about the exact nature of the stimuli and the experimental paradigm in which the response occurred[68]. The main drawback of the EDA system is that it is a slow response system, the typical latency in the response being 1-3 seconds. Hence it is not suitable for tracking an emotional stimulus that progresses very rapidly[68].

4.1.3 Respiration

Respiration has been used extensively as an indicator of emotional states, stress, arousal and mental load[19].

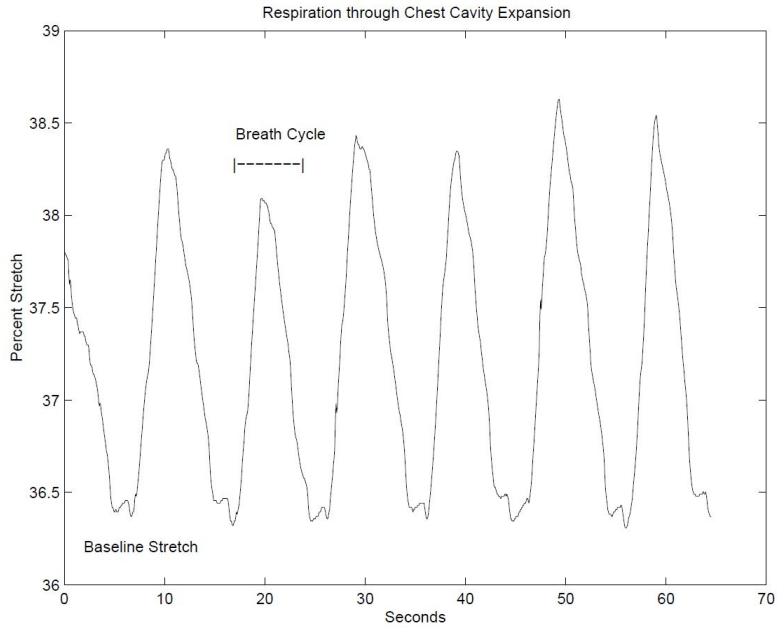

Figure 4.1.5: The respiration signal
(source:[41]). The figure shows the inhalation and exhalation pattern obtained from a hall effect sensor inside an elastic tube streched across the diaphragm.

The respiratory cycle consists of an inspiration phase, followed by an expiration phase. In [69] three features derived from respiration are described: the respiration rate, respiration amplitude and the inspiration-expiration ratio. Roscoe [19] and Haward [70] have studied respiration as an indicator of stress in aviation scenarios. Wientjes [71] is of the opinion that *'the respiratory pattern primarily varies along a continuum that ranges from excited and action-oriented states, via attentive, alert states, to inhibited or low arousal.'* Furthermore, he makes the following observations based on the morphology of the breathing cycle:

1. Rapid shallow breathing

   This breathing pattern is described as an increase in the respiration rate and a reduction in amplitude of respiration. This pattern is correlated with a attention and alertness. Emotionally this pattern can indicate affect states varying from 'tension' to 'anxiety'.

2. Rapid deep breathing

   Involving high respiration rate as well as high amplitude of respiration, it is characteristic of scenarios involving intense tension, but without the control aspect. Typical of aroused states involving *'unrestrained or massive action orientation'*(i.e., fight or flight).

3. Slow shallow breathing

   Characterised by a lower respiration rate and low amplitude of respiration, this process is indicative of a *'withdrawal from the environment'* state. Thus it may be categorical of either grief/depression or calm-happiness and satisfaction.

4. Slow deep breathing

   Low rate of respiration as well as a lower amplitude of respiration. This pattern indicates resting state or deep relaxation.

4.1.4 Electromyographic (EMG) Activity

The electromyograph (EMG) measures the muscle activity by detecting surface voltages that occur when a muscle is contracted[41].

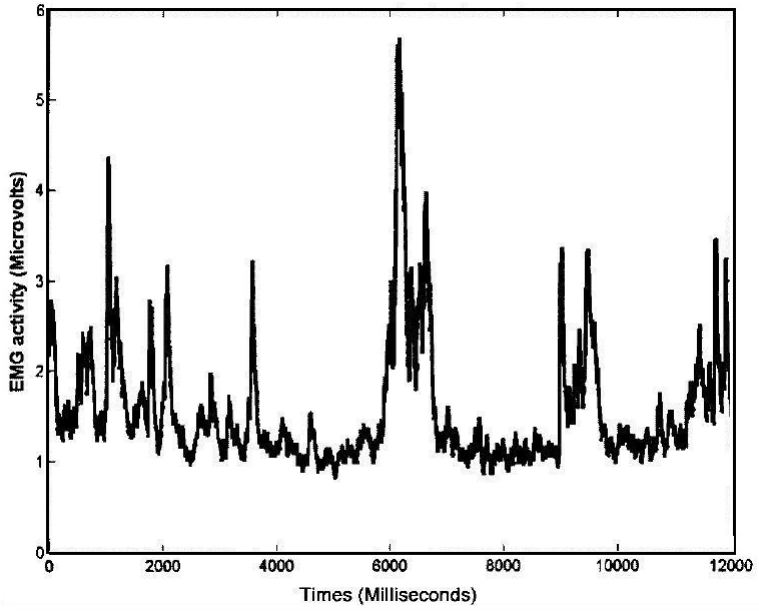

Figure 4.1.6: A typical facial EMG signal (RMS valued)

(source:[35])

According to Tomkins [72] *'affect is primarily facial behaviour'* and emotions are effectively communicated through facial expressions. Following this presumption the two main facial muscle sites active during an emotion expression state are[73]:

1. The *corrugator supercilli* - These muscles knit the eyebrows during a frown.

2. The *zygomaticus major*- These muscles elevate the lips to form a smile.

Significant corrugator activity is observed with decrease in valence (Fig.3.1.1) and high zygomaticus activity is associated with increase in valence of an emotion episode [74],[75],[76].

4.1.5 Temperature

Decrease in skin temperature during episodes of negative emotions (fear, anger etc.) have been reported by Levenson et al.[77]. Similarly Vos et al. [78] reports higher skin temperature during the expression of low intensity negative emotions compared to the expression of low intensity positive emotions.

In this chapter a review on the physiological signals commonly used in affect computing was presented. Conclusive evidence exist in literature to support the applicability of physiological signals for affect state estimation. For the same reason these signals are utilised as input parameters in the proposed experiment for affect state estimation.

Part II

Design of the Experiment

Chapter 5

Affect State Estimation from Video Stimuli

5.1 Introduction

In this chapter the experiment undertaken for affect state estimation in the context of the DLR-RMS is detailed. This experiment is the first among a series of tests to be conducted at the DLR for affect state estimation studies in motion simulation and forms the crux of this thesis.

It was envisioned that the experiment be first developed 'on ground'-i.e., without involving motion. This decision was motivated by the following reasons:

1. Validation of knowledge from literature study- An 'on ground' experiment will help to replicate the test conditions prevalent in most of the research work introduced in section 3.2.1 and the results acquired during the same can be compared with the results from similar researches. Thus the experiment can serve as a basic framework which can be later extended into the simulator.

2. Improvement in the robustness of the system- Not all physiological responses introduced in chapter 4 might be required for accurate affect state estimation. Some of the sensors might provide redundant information which can be identified during the 'on ground' experiment. The set up thus can be made robust before being transferred to the DLR-RMS.

5.2 Aim

The aim of the experiment is to provide a means for mapping the expressed affect states to the corresponding changes in the physiological parameters. Here the focus is on studying the probable affect states induced during a motion simulation scenario aboard the DLR-RMS, in a

static set up (i.e., without involving motion) from video segments acting as stimuli.

The anticipated affect states in the context of the DLR-RMS can be broadly concluded to just 4 representative and contrasting classes. They are:

1. Thrill
2. Fear
3. Boredom
4. Calmness

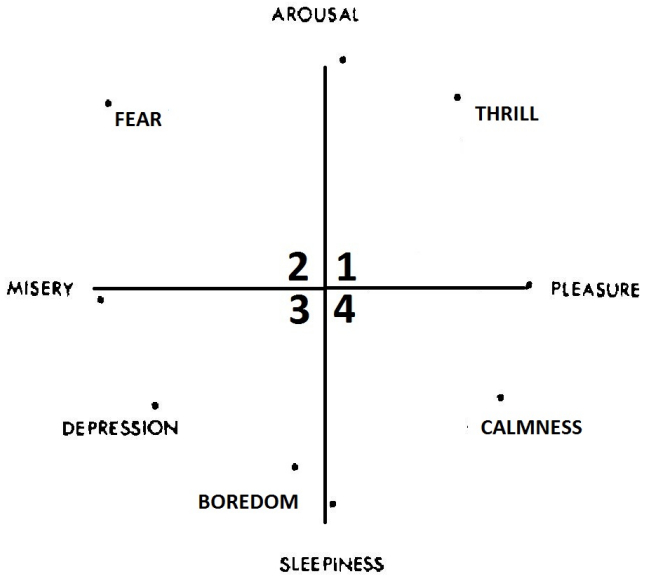

Figure 5.2.1: The Valence-Arousal model (VA) by Russell.
The dimensions of Arousal is marked on the vertical axis and valence is marked along the horizontal axis. (source:[79])

In the figure 5.2.1, it can be seen that 'Thrill' scenarios are classified as high valence and arousal events. Thus they lie in the first quadrant. 'Fear' scenarios denote events associated with high arousal and very low valence. Hence 'Fear' scenarios are representative of the second quadrant. 'Boredom' scenarios are suggestive of events that elicit very low arousal and neutral or low valence. They thus lie in the third quadrant near the neutral (neither high nor low) axis of valence.'Calmness' scenarios lie in the fourth quadrant and are representative of events with intermediate levels of valence and arousal.

The reduction of the affect states as described is based on the following proposition:

Given the context of a motion simulation scenario aboard the DLR-RMS, it is reasonable to assume that the affect states *will fall* into one of the four categories described in the last

paragraph. Furthermore these affect states are well differentiated in the valence-arousal space (see figure 5.2.1). By the application of suitable stimuli, distinct and characteristic physiological responses can be obtained which can be used for studying the underlying affect states.

Affect state	Definition as per dictionary	Dimensions in Valence-Arousal space	
		Valence	Arousal
Thrill	A feeling of extreme excitement, usually caused by something pleasant[80].	++	++
Fear	A strong emotion caused by great worry about something dangerous, painful,or unknown that is happening or might happen[81].	– –	++
Boredom	The state of being weary and restless through lack of interest[82].	n	–
Calmness	Not affected by strong emotions such as excitement, anger, shock, or fear[83].	+	+

Table 5.1: **The meanings of the intended affect states in a dictionary.**
Note that each word is rather an umbrella construct, representative of all terms of similar interpretation. Hence the construct 'Thrill' encompasses similar terms like 'Excited', 'Delighted', 'Amused' etc. and the construct 'Fear' include terms like 'Alarmed', 'Tensed', 'Afraid' etc. See [79].
+ denotes a high value of the respective facet, and ++ a very high value. Similarly, – denotes a low value of the respective facet, and – – a very low value. n is 'neutral' i.e., neither high nor low.

5.3 Structure of the Experiment

Based on criteria mentioned in the last sections, we decided that the experiment be formulated to have the following attributes (Fig,5.3.1):

1. Inducement of the intended affect state - This is achieved by introducing the subject to a properly designed stimuli. Stimuli in this experiment are video segments.

2. Measurement of bio-signals - The physiological features described in chapter 4 are measured and recorded by means of a suitable data acquisition system.

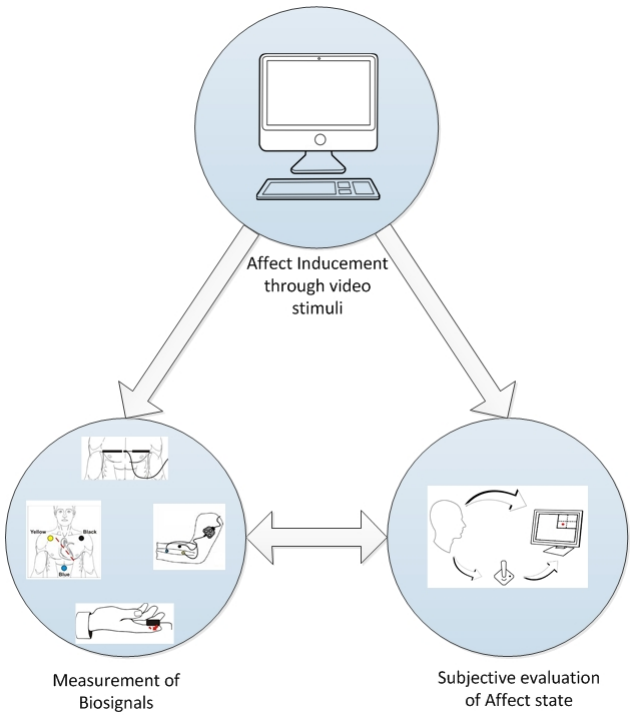

Figure 5.3.1: The structue of the proposed experiment

3. Subjective evaluation of the affect state- The subject evaluates the particular affect state experienced by him/her by means of a labelling interface employing a joystick as an input device.

The basic framework of the proposed experiment for affect state estimation was discussed in this chapter. The experiment is executed through different modalities as described in section 5.3. A detailed discussion of these modalities is presented in the subsequent chapters.

Chapter 6

Video Segments as Stimuli

In this chapter design of the stimuli set, the data acquisition system and the labelling interface are elaborated in detail.

6.1 Video segments as stimuli

The scope of using movie segments as affect eliciting stimuli has been studied by many researchers. According to Gross et al., *'films have the desirable properties of being readily standardized, involving no deception, and being dynamic rather than static. Films also have a relatively high degree of ecological validity, in so far as emotions are often evoked by dynamic visual and auditory stimuli that are external to the individual.'*[84] The challenge here is to identify film segments that elicit the probable affect states aboard the DLR-RMS in sufficient intensity and in a sustained and discrete manner (i.e., the film segment should elicit the intended affect and that alone for most of its duration). There has already been research in this direction and several film-stimuli set for induction of basic emotions by [84], [85], [86]. In the scope of this experiment 8 video segments were selected to induce the intended affect states. The video segments were selected from a pool of video segments collected from the data base proposed by [84] and from collective internal evaluation of the project team.

6.2 The Film-Stimuli Set

The final video stimuli set consist of eight video segments to act as the stimuli for affect state induction. The video segments included 2 movie segments (genre 'comedy') to elicit the affect state of thrill, 2 film segments (genre 'horror') to evoke the affect state of fear, 2 movie segments (genre 'documentary') to evoke the affect state of boredom, and 2 video segments (genre-wildlife documentary) for 'calmness'. The length of the video segments varied from 120 seconds to 197

seconds with an average length of 158 seconds. From the video stimuli set video sequences were created for each test subject by combining the different video-stimuli in a pseudo-random fashion to mitigate the effects of confounding in the experiment[87]. The video segments were also interleaved with 'blue screens'[4] which marked the transition state between the film clips and had duration of 120 seconds. The set also consisted of an introductory video clip (genre-documentary) which elicits mild positive emotions. This is done in order to accustom the subject to the procedure, and to wear out the initial 'excitement' about the experiment that might give erroneous data[84]. It was also ensured that no two video segments corresponding to the same genre appeared in succession[84].

Video segment	**Intended affect**	**Genre of the segment**	**Clip length**
Introductory video segment	Random affect	Nature documentary	101 sec
Blue screen	Transition phase	Blue screen	120 sec
Amusement-1	Thrill	Comedy	185 sec
Amusement-2	Thrill	Comedy	173 sec
Fear-1	Fear	Horror	197 sec
Fear-2	Fear	Horror	144 sec
Boredom-1	Boredom	Monologue	119 sec
Boredom-2	Boredom	Monologue	160 sec
Calmness-1	Calmness	Nature documentary	145 sec
Calmness-2	Calmness	Nature documentary	147 sec

Table 6.1: **The video stimuli set.**
The table shows a summary of the 10 video segments selected for the experiment. These video segments were combined in a pseudo-random fashion to obtain unique video sequence for each test subject.

6.3 The Labelling System

The conventional methodology for acquiring subjective assessment in affect estimation studies include answering questionnaires [88], Likert scale ratings[84], or more recently graphical UIs[89]. All these methods introduce the following errors in the subjective evaluation:

1. Errors due to distraction- The experiment has to be interrupted at intervals for answering the questionnaires and this causes distraction to the test subject. Also the act of repeated measurements can potentially alter the emotional response[88]. Therefore a continuous evaluation system without obvious interference is preferred.

2. Errors due to discretisation of evaluation- The conventional methods make continuous evaluation of stimuli impossible. The user is asked to provide a single emotional rating for

[4]Bluescreen- A blank scene of blue colour, used to denote no activity.

a stimulus that had emotional events of varying magnitude and this leads to generalisation of the response. In the case of video stimuli, these methods hardly reflect the dynamic nature of the stimuli. A better alternative would be to use a system that allows continuous evaluation, in the same temporal space as the stimulus occurs[90].

3. Errors due to temporal latency- Retrospective emotion recall is less accurate than immediate reports [90]. Therefore even a short delay between the activation of emotion and the self-report can lead to erraneous responses[88]. Hence a system that allows real time evaluation should be used in the context of affect estimation studies.

A labelling system employing a joystick as a user input device was developed for subjective evaluation of affect state to solve the drawbacks of the conventional methods and is a novelty of this research work. It allowed continuous measurement/recording of the user response with least interference and temporal latency. The applicability of this labelling interface was also evaluated by means of a 'system usability scale' survey [91]. The System Usability Scale (SUS) is an effective tool for assessing the usability of products and services including interfaces, response systems and applications [92]. The SUS is composed of ten statements pertaining to the effectiveness of the product being tested, each having a five-point Likert scale that ranges from 'Strongly Disagree' to 'Strongly Agree'. In this experiment the 'All Positive SUS' developed by Jeff Sauro was used [91] (See Appendix A for details).

6.4 The Labelling UI

The labelling UI is implemented through the hardware and software components.

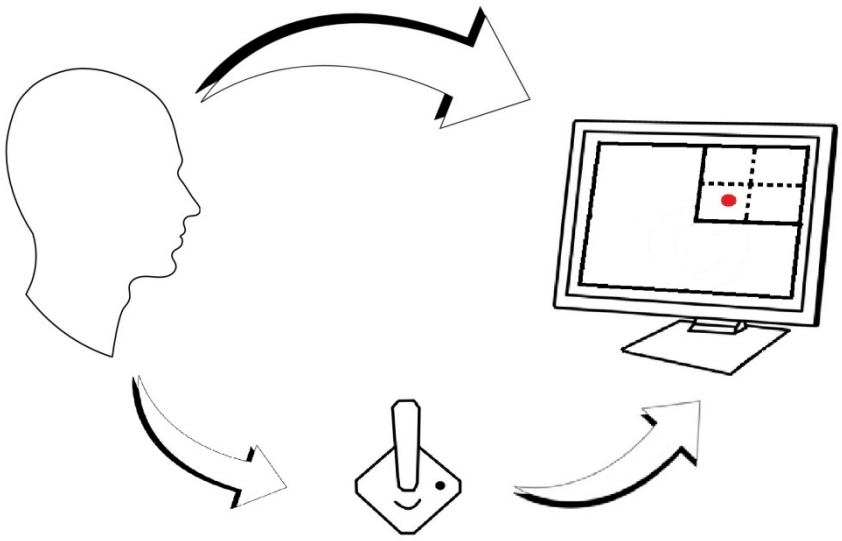

Figure 6.4.1: The joystick interface system

The hardware component is the physical component through which control of user choice is achieved. In this case it is represented by the joystick itself.

The software component is represented by the graphical interface using which the subject expresses his choice. This is essentially a visual interface where the user navigates the joystick pointer to the appropriate region on the interface screen. In the context of this experiment the affect state of the user was to be evaluated. This was achieved by designing the interface on a 'valence-arousal space' using the self assessment manikins (SAM).

As explained in section 3.1 the affect state of an individual can be described in a two-dimensional space as coordinates of affective valence and arousal. This means that a simultaneous mapping of these two components can lead to the successful recognition of affect state experienced by a person. The affective dimensions of valence and arousal are expressed by self assessment manikins (SAM) in the graphical interface. The Self-Assessment Manikin (SAM) is a non-verbal pictorial assessment technique that directly measures the pleasure and arousal associated with a person's affective reaction to a wide variety of stimuli[93].

On the valence axis, the SAM ranges from a happy smiling figure denoting the highest level of pleasure to a frowning unhappy figure representing the least level of pleasure. The SAM figure in the middle denotes a neutral phase of valence i.e., neither in a state of pleasure nor displeasure. Similarly on the arousal axis the SAM figure ranges from an excited, wide-eyed figure with an exploding starburst in the centre, denoting the affective state of maximum arousal to a sleepy figure with the starburst reduced to a dot and closed eyes, denoting the least levels of arousal. The neutral state of arousal is represented by the SAM figure in the middle. We employed a 9 point SAM system; i.e., the subject can choose any of the five figures as well as between any two figures on each scale for representing his/her affect state.

On the graphical interface for affect estimation, the valence dimension is represented in the horizontal axis and the arousal dimension along the vertical axis, as shown in the figure 6.4.2. The joystick is centered at (5,5) representing a neutral affect state in terms of valence and dimension. The user is free to move the joystick point to any position in the graphical interface that best describe the affect state at the time. These positions are mapped to the equivalent ratings of valence and arousal in the range [0.5 9.5] by using suitable transfer functions which are determined by the geometrical coordinates of the labelling interface.

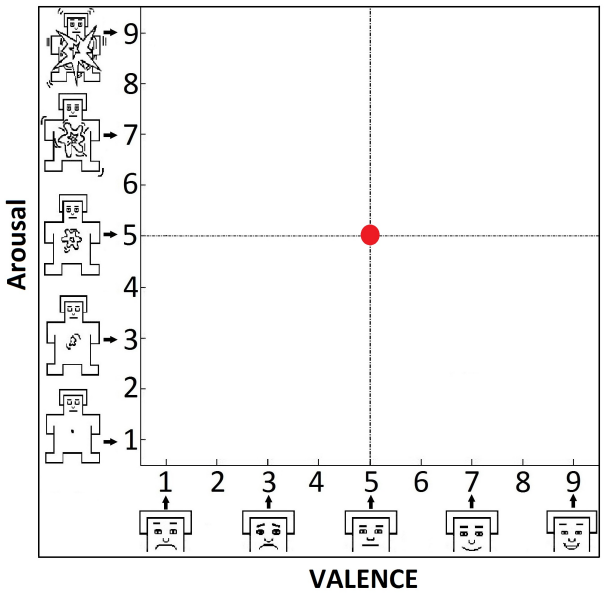

Figure 6.4.2: The user interface

The graphical interface is displayed over the video during the experiment as shown in the figure 6.4.3

Figure 6.4.3: The video with the user interface display

6.5 Data Acquisition - System and Procedure

In this section the data acquisition system adopted for data collection are detailed.

6.5.1 Instrumentation

The instrumentation architecture for the measurement of bio-signals is as shown in figure 6.5.1

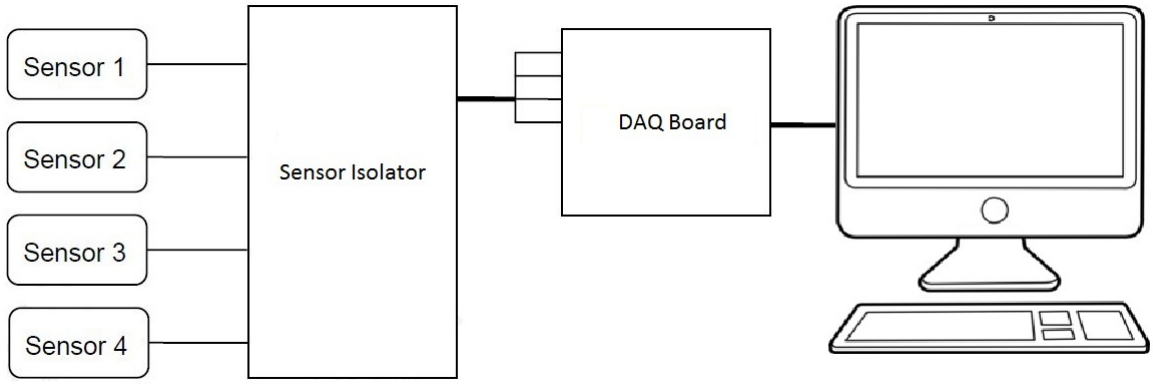

Figure 6.5.1: The instrumentation architecture developed for affect estimation

The main components of the data acquisition system are the Biosensors, the Sensor Isolator and the Data Acquisition module.

6.5.1.1 Biosensors

The bio-signals were measured using the sensors from Thought technology Ltd.[94]. Seven sensors were used to measure the physiological features described in chapter 4. They are: ECG sensor, BVP ensor, EDA sensor, Respiration sensor, Temperature sensor, and 2 EMG sensors for measuring the muscular activitiy of the corrugator supercilli and zygomaticus major muscles.

6.5.1.2 Sensor Isolator

To ensure electrical safety in the instrument setup the manufacturer [94] recommends the use of a 'sensor isolator' box when interfacing subjects connected with sensors to line powered equipment. The Sensor Isolator is an interface device providing medical grade electrical isolation between the subject-connected sensors and the acquisition system. The sensor isolator ensure that the sensors are safely interfaced to the analog inputs of line-powered systems such as computers and other data acquisition modules.

6.5.1.3 Data acquisition module

The bio-sensors are interfaced to an NI 9205 data acquisition (DAQ) device from National Instruments. It features 16 differential analog inputs with 16-bit resolution and a maximum sampling rate of 250 kS/s [95].

6.6 Data Acquisition Program

The data acquisition application for the experiment was implemented in LabVIEW 2013[96]. The application follows the state machine architecture (Fig.6.6.1).

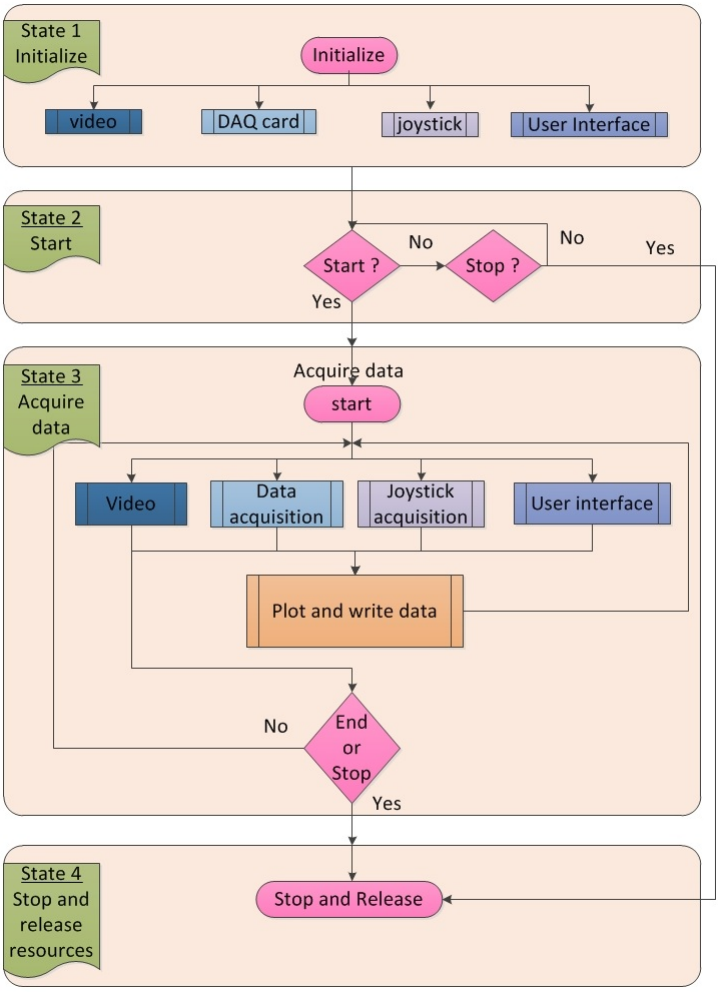

Figure 6.6.1: The state Machine architecture developed for the experiment

6.6.1 State 1-Initialize

The initialization of the video, data acquisition card, and the user interface is done in the first state (Fig.6.6.2).

6.6.2 State 2-Start

When the subject is ready, a start button is pressed which leads the program to the next state. There is also an option to stop the experiment at this stage.

6.6.3 State 3-Data Acquisition

Once the start button is pressed, the video, the labelling interface and the data acquisition from the sensors and the joystick begin simultaneously. The data was acquired at 1 kHz for the sensors and at 20 kHz for the joystick . The data from the sensors and the joystick are plotted and written to measurement files. This state continues until the video (which is the master

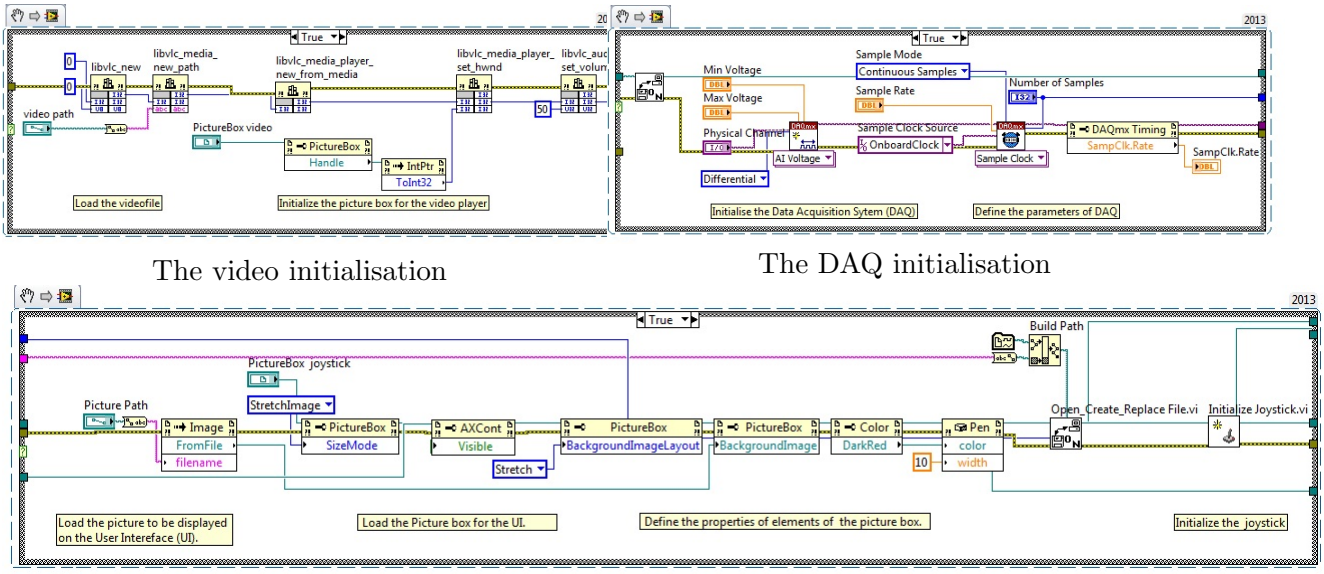

Figure 6.6.2: The joystick interface initialisation and the DAQ initialisation implemented in LabVIEW

process) stops or the stop button is pressed (Fig.,6.6.3).

6.6.4 State 4-Stop and Release

When the video stops or when the stop button is pressed, the program stops and all the resources are released.

The instrumentation architecture of the experiment was discussed in this chapter. The hardware components of the experiment setup was discussed in detail. The program used for the implementation of the labelling interface and data acquisition were also discusssed. In the next chapter the procedure followed for the experiment is discussed in detail.

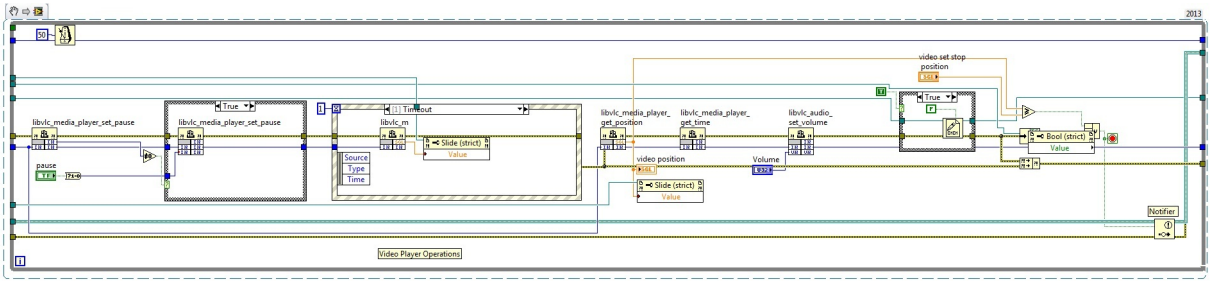

The video system

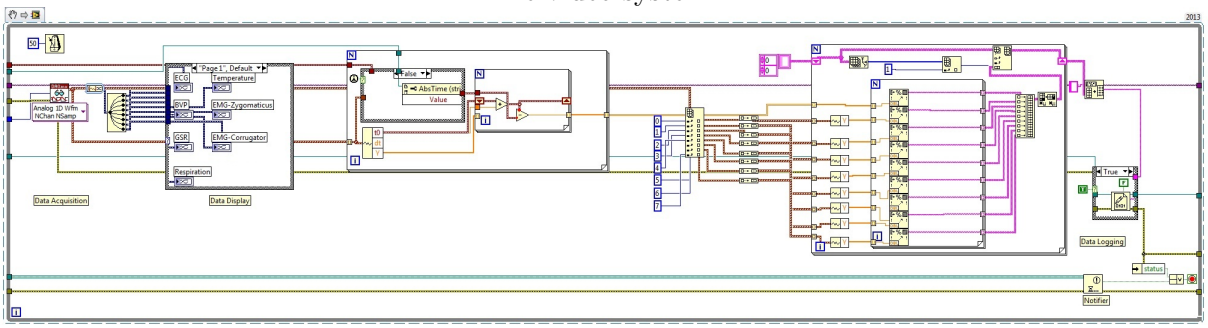

The DAQ measurement and logging

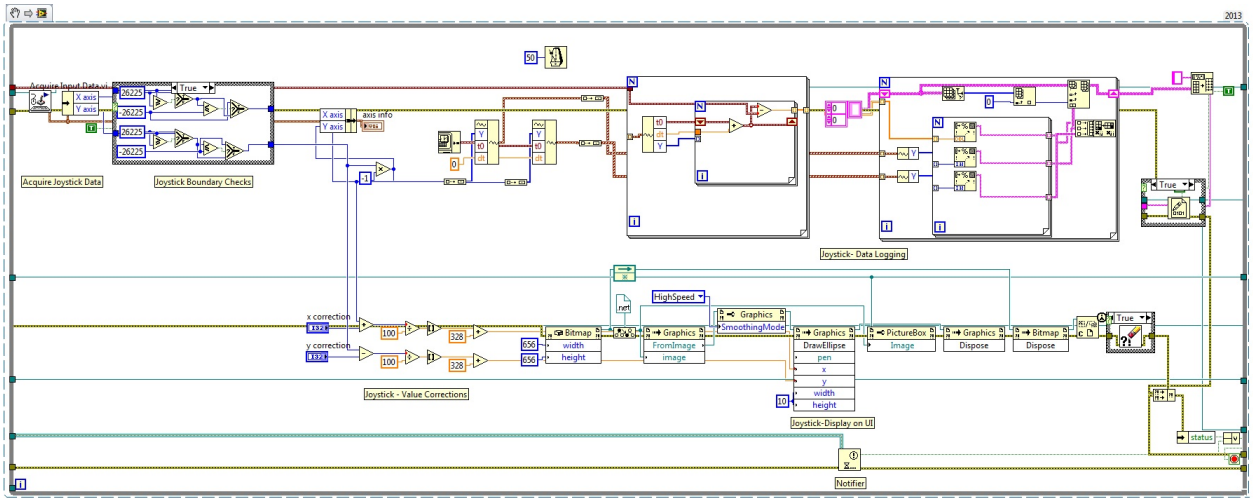

The UI display and logging

Figure 6.6.3: The data acquisition state implemented in LabVIEW

Chapter 7

Experiment procedure

7.1 Participants

30 volunteers (15 male, 15 female); average age: 27.2 years; standard deviation 4.4 years; range: 22-37 years) belonging to different ethnic groups participated in the experiment. The subjects also signed an informed consent form. All subjects were instructed in English and all subjects spoke English as their first or second language.

7.2 Environment

The subject sat in a chair with their hands resting comfortably on tables on either side. The subject operated the joystick for the labelling interface using the dominant hand. The chair was set at a comfortable viewing position from a 42" 16:9 flat panel screen attached to the wall. The room was silent and darkened for an enhanced viewing experience. Superior quality headphones were provided to ensure the best sound effects.

7.3 Sensors

7.3.1 The ECG sensor

The ECG sensor is a pre-amplified electrocardiograph sensor that detects the electrical signal generated by the heart muscles during contraction. The electrical signal propagated throughout the body is captured by the electrodes, amplified and filtered by the sensor before converting into a digital signal by the encoder.

7.3.1.1 Placement of the sensor

The electrodes are placed in a triangular configuration on the chest as illustrated in figure 7.3.1. The yellow and blue electrodes are placed parallel to the heart's main axis, over the right and left coracoid processes and the blue electrode over the xiphoid process [97].

7.3.1.2 Preparation of the site

The electrode sites for ECG placement are prepared to minimize artifacts by gently abrading the skin surface to remove dead skin, oil and sweat. The site is then cleaned and dried using an alcohol pad. Pre-gelled electrodes are fixed firmly on the skin and the lead cables are connected[98].

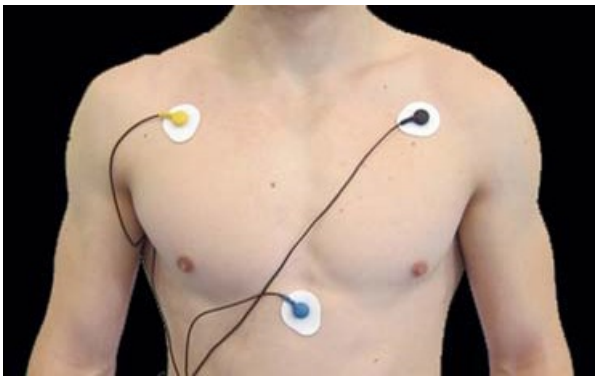

Figure 7.3.1: The ECG electrode position
(source:[99])

7.3.2 The BVP sensor

The blood volume pulse (BVP) sensor used is a photoplethysmograph housed in a small package worn on a finger. It measures the relative amount of blood flow through tissue using a photoelectric transducer.

7.3.2.1 Placement of the sensor

The sensor is placed against the fleshy part of the first joint of the left middle finger [99] (Fig.7.3.2).

Figure 7.3.2: The BVP sensor position
(source:[94])

7.3.2.2 Preparation of the site

No specified preparation of the skin is required since the BVP sensor detects the back-scattered infrared light. However it is advisable to make sure that the subject washes the hands so that dirt does not obstruct the sensor's transducer window. The sensor is firmly attached using an elastic band or Coban tape. It is also ensured that no ambient light enters into the photo detector window of the sensor. Measures are taken to minimize artifacts introduced due to ambient temperature, excessive pressure on the finger and sympathetically mediated vasoconstrictions as per the instructions in [99].

7.3.3 The Electrodermal Activity (EDA) sensor

The Skin Conductance Sensor measures the electrical conductance (electrodermal activity) between two points on the skin (see section 4.1.2).

7.3.3.1 Sensor placement

To measure skin conductance a bipolar placement of silver-silver chloride electrodes on the 2^{nd} and 3^{rd} fingers of the non dominant hand is followed.

7.3.3.2 Preparation of the site

The skin surface is mildly washed using water. Use of an anti-bacterial soap or alcohol based sanitizer is not recommended as this may lead to excessive drying of the skin resulting in artifacts. Conductance gel is applied to the electrode site and the electrode bands are firmly fixed to the fingers. Since the degree of hydration and electrolytic concentration in the skin surface influence the electrodermal activity, sufficient time is allowed (typically 5 to 15 minutes) before commencing the experiment, to stabilize the skin-electrolyte interface[100][98]. The sensor sensitivity is checked before the commencement of the experiment by asking the subject to take

a deep breath and hold it for few seconds. A good electrodermal signal shows a change in response[98].

Figure 7.3.3: The skin conductance sensor position
(source:[94])

7.3.4 The Respiration sensor

The respiration sensor detects breathing by monitoring the expansion and contraction of the chest cavity using a Hall effect sensor attached around the chest using a velcro band.

Figure 7.3.4: The respiration sensor position
(source:[94])

7.3.4.1 Sensor placement

The respiration sensor belt is placed high on the torso immediately under the arms and above the breasts and the tautness needs to be comfortable for the subject[98].

7.3.4.2 Preparation of the site

No site preparation is required.

7.3.5 The Temperature sensor

Temperature sensor measures skin surface temperature between 10°C - 45°C. It is an epoxy rod thermistor which detects very small changes in skin temperature and converts them into an electrical signal.

7.3.5.1 Sensor placement

The sensor is fixed firmly to the pinky finger of the left hand using Coban self-adhesive tape. It is ensured that the sensor makes good contact with the finger.

7.3.5.2 Preparation of the site

No site preparation is required.

Figure 7.3.5: The temperature sensor position
(source:[94])

7.3.6 The EMG sensor

The electromyograph sensor (EMG) is a differential amplifier which measures the surface voltage associated with the contraction of the muscle.

7.3.6.1 Sensor placement

Two sets of EMG sensors were used to measure the muscular activity at two locations. The sensors are placed following the guidelines from [75].

1. Corrugator supercilli muscles
   One electrode is affixed directly above the brow on an imaginary vertical line that traverses the endocanthion (the inner commissure of the eye fissure). The second electrode is positioned 2 cm lateral to, and slightly superior to, the first on the border of the eyebrow (Fig.7.3.6). The third electrode (reference electrode) is placed at a convenient position on the body [101].

2. Zygomaticus major muscles
   One electrode is placed midway along an imaginary line joining the cheilion and the preauricular depression (the bony dimple above the posterior edge of the zygomatic arch), and the second electrode is placed 1 cm inferior and medial to the first (i.e., toward the mouth)

along the same imaginary line (Fig.7.3.6). The third electrode (reference electrode) is placed at a convenient position on the body [101].

7.3.6.2 Preparation of the site

Skin preparation include gentle abrasion of the skin to lower the inter electrode impedance to 5 - 10 kilo Ohms. Pre-gelled electrodes are then firmly fixed on the sites and the cables to the sensor connected to these electrodes[75].

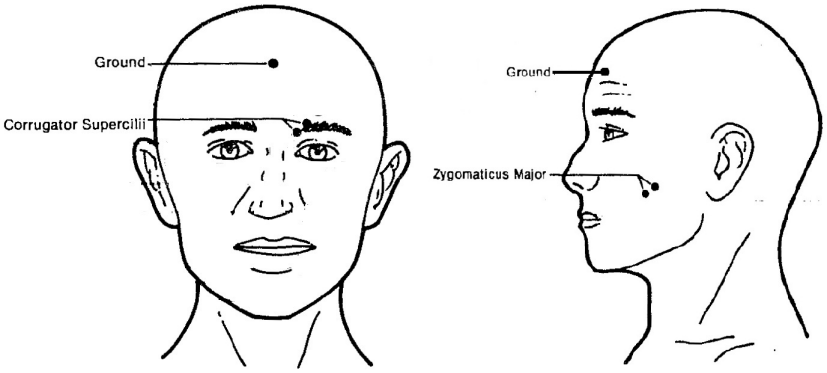

Figure 7.3.6: The EMG sensor position
(source:[75])

7.4 Procedure

The subjects were previously informed about the experiment in general, without revealing the exact research goals. An experiment session began by signing the informed consent form. Instructions were then provided on how to use the user interface system as explained in section 6.3 for subjective evaluation. Any doubts on the part of the subject about the usage of the labelling system were cleared and the sensors were fixed on the subject as explained in section 7.3 to the non-dominant side of the body. The measurements from the sensors were checked and corrections were made whenever required.

Figure 7.4.1: The sensors attached on the test subject

The subject was instructed to watch the video carefully and rate their *'feeling at the moment'* using the joystick interface. It was stressed that *'they are expected to rate their feelings while watching the video, and not the emotional (affect) content of the video itself. They were also asked to maintain the joystick location as long as they felt the same feeling*[5] *and that they do not have to change with every scene or event in the video clip'*. A video sequence consisting of 5 practice video clips belonging to different affect classes were first shown to the subject to accustom him/her to the nature of the experiment. The subject used the joystick based interface for self-reporting during this practice session and the experiment superviser evaluated if the subject really understood the operation of the interface and corrected whenever necessary. It was also instructed that they could shut their eyes or look away if they found any segment as too disturbing. After the training phase, the experiment was initiated. The duration of the main video phase was 40 minutes. After the completion of the test general verbal feedback on their experience during the test was taken. The subject was also asked to respond to the System Usability Scale (SUS) questionnaire (see section 6.3). At the end of the test the sensors were removed and refreshments were offered.

In this chapter the experimental procedure adopted for the acquisition of the physiological signals for affect state estimation was discussed. Various features are extracted from these signals relevant in the context of affect computing. The extraction of these features, analysis and the results derived are explained in the subsequent chapters.

[5]The term 'affect' was not used while conversing with the subjects, rather the term 'feeling' was used to convey the meaning.

Part III

Data Analysis

Chapter 8

Feature Extraction

A number of features can be extracted from the measured biosignals for affect state estimation. Table 8.1 summarizes the common physiological signals and the features derived from them in affective computing.

In this chapter the feature extraction procedure applied to the various biosignals is detailed. All the signal processing and analysis was implemented in Matlab[102].

8.1 Biosignals-Feature Extraction

8.1.1 ECG Feature Extraction

The features extracted from the ECG data are the interbeat intervals (IBI) and the heart rate (HR) (see section 4.1.1). The Hamilton and Tompkins algorithm for QRS detection [103] is used to calculate the interbeat interval. The source code was adapted from Sedghamiz [104].

The first step in ECG feature extraction is the identification of time locations of the QRS component in the ECG signal. The QRS detection is implemented in three steps:

8.1.1.1 Preprocessing

The preprocessing step involves band-pass filtering of the signal with cut-off frequencies 5 and 15 Hz to get rid of the baseline wander and muscle noise (Plot:2, Fig:8.1.1).

8.1.1.2 Non-linear Transformations

Then the filtered signal is derived using a derivative filter to enhance the higher frequency QRS components. The signal is then squared to enhance the dominant peaks. It is then smoothed using a moving average window of length 30 ms.

Physiological response	Features Extracted	Unit
Cardiovascular activity (Electrocardiogram (ECG) or Blood Volume Pulse (BVP))	Heart rate (HR)	beats/min
	Mean of inter beat interval (IBI)	s
	Standard deviation of inter beat interval	s
	Low Frequency (LF) power (0.05Hz - 0.15Hz)	ms^2
	High Frequency (HF) power (0.15HZ - 0.40Hz)	ms^2
	Very Low Frequency (VLF) power (less than 0.05Hz)	ms^2
	Ratio of powers LF/HF	No unit
	Mean amplitude of the peak values of the BVP signal	µV
	Standard deviation of the peak values of the BVP signal	µV
	Mean pulse transit time	ms
Electrodermal Activity (EDA)	Mean tonic activity level	µS
	Slope of tonic activity	µS/s
	Standard deviation of tonic activity	µS
	Number of skin conductance responses	nr / min
	Mean amplitude of skin conductance response (phasic activity)	µS
	Maximum amplitude of skin conductance response (phasic activity)	µS
	Rate of phasic activity	Response peaks/second
	Skin conductance response half recovery time	s
	Skin conductance response rise time	s
Respiration	Respiration rate	nr/min
	Amplitude	%
Muscle activity (EMG of corrugator and zygomaticus muscles)	Mean of muscle activity	µV
	Standard deviation of muscle activity	µV
Skin temperature	Mean of skin temperature	°C
	Standard deviation of skin temperature	°C

Table 8.1: **Summary of the features derived from biosignals.**
The table summarizes the most common features extracted from the biosignals (source:[105], [26])

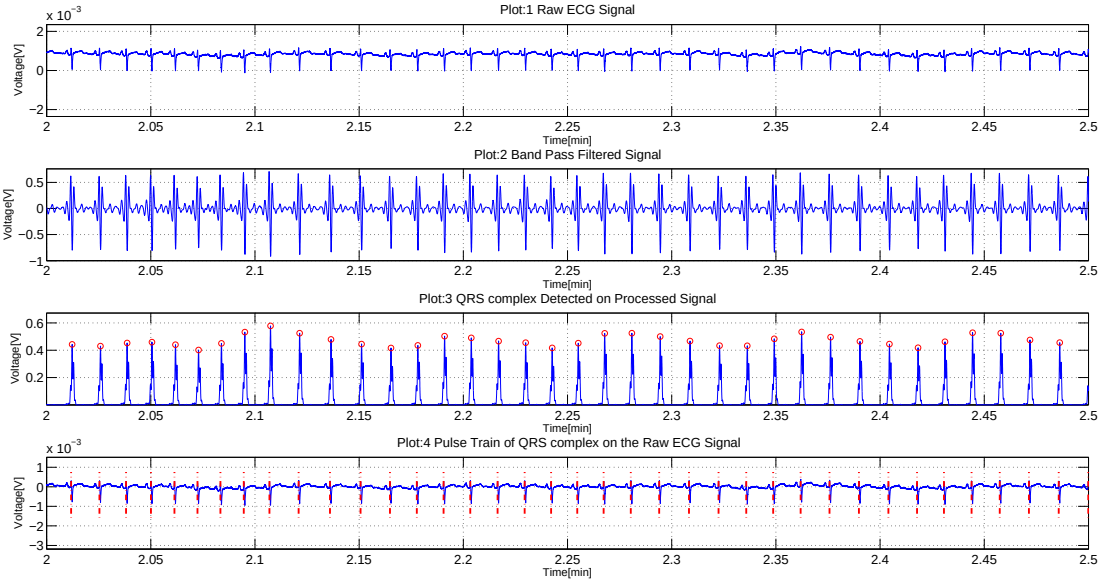

Figure 8.1.1: Interbeat intervals from the ECG signal

8.1.1.3 Peak Detection

The peaks which correspond to the QRS component in the signal are detected using a peak detection algorithm. The algorithm also adapts the threshold values for peak detection in accordance with the changing signal quality (Plot:3, Fig:8.1.1).

8.1.1.4 Decision Rule Algorithms

Decision rules are applied to avoid detecting multiple peaks in a single heart beat (induced by motion artefacts or the T component of ECG wave), and to detect missed peaks. Multiple peak detection is avoided by enforcing a time delay of 200 ms between 2 peak detections. This is based on the fact that a ventricular depolarization cannot occur in less than 200 ms from a previous one, despite a stimulus [106]. T wave discrimination is enforced by comparing the mean slope of the waveform with a previously detected peak. The slope of the slow changing T wave is much lower than that of a QRS component. The algorithm also performs a 'searchback' if a long period has transpired (1.66 times the current R-R interval) without activity, to account for missed beats (Plot:4, Fig:8.1.1).

8.1.1.5 Heart Rate

The heart rate is calculated as the reciprocal of the interbeat intervals [61] (figure 8.1.2).

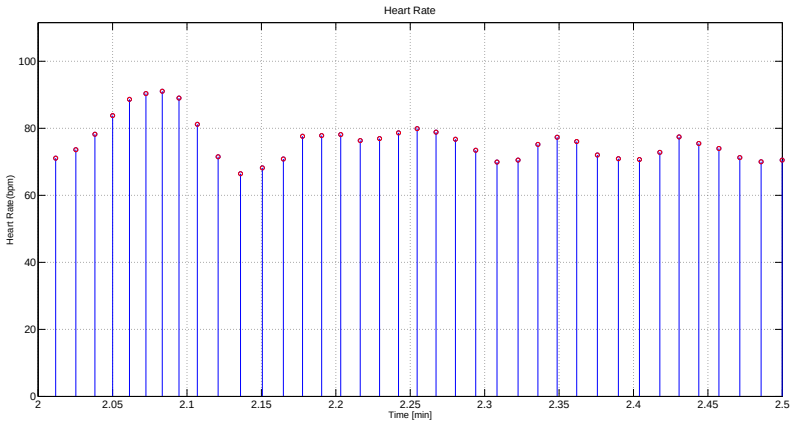

Figure 8.1.2: Heart rate extracted from the ECG signal

8.1.2 BVP Feature Extraction

The BVP signal provides an alternative way to estimate the heart rate as explained in section 4.1.1. Heart rate is calculated from interbeat interval obtained from the BVP waveform. The raw BVP signal is first low pass filtered at 5 Hz to remove the high frequency noise (induced primarily due to motion artefacts) and then high pass filtered at 0.5 Hz to remove the baseline wander (induced primarily due to respiration) [107]. An adaptive peak identification algorithm was used to detect peaks corresponding to each pulse in the filtered signal (Plot:2, Fig.8.1.3). The detection of the dichrotic notch in the signal is avoided by enforcing a time interval of 550 ms (the minimum width of a single pulse) between 2 adjacent peaks [108].

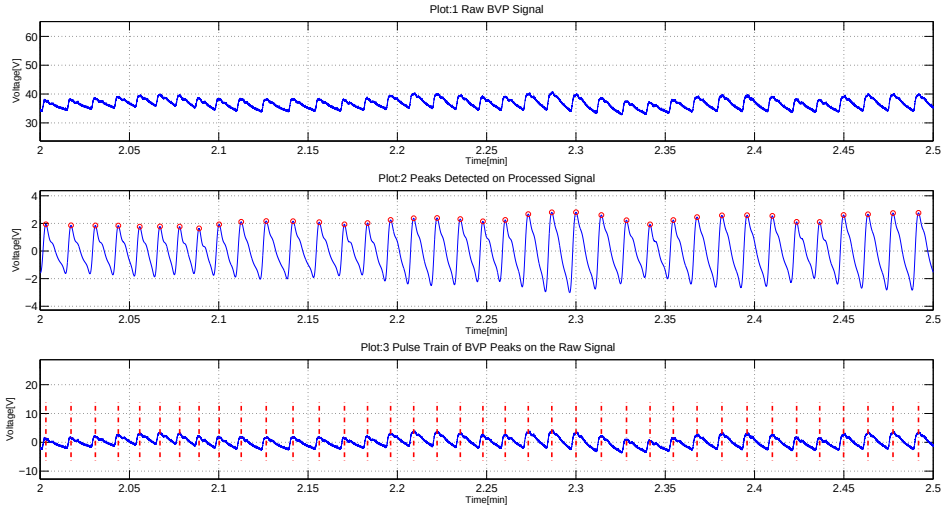

Figure 8.1.3: Interbeat intervals from BVP signal

8.1.2.1 Heart rate

As with the ECG data the heart rate is extracted from the BVP signal as the reciprocal of the interbeat intervals (figure 8.1.4).

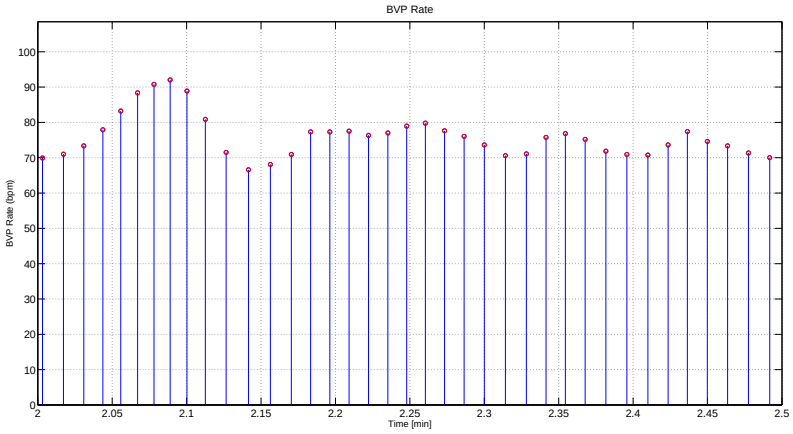

Figure 8.1.4: Heart rate from BVP signal

8.1.3 Electrodermal Activity Feature Extraction

The features extracted from the skin conductance sensor are the tonic and phasic components (see section 4.1.2).

The raw signal was first low pass filtered at 15 Hz to remove the high frequency noise. The following procedure was then applied to derive the tonic and phasic components[100]:

1. Calculation of the signal's minima by a moving window of length 5 seconds over the whole signal.

2. Smoothing of the minima curve by means of a moving average window of length 5 seconds, to eliminate the sharp peaks. This represents the tonic component of the signal (plot:2, fig:8.1.5).

3. The tonic component is then subtracted from the raw signal to obtain the phasic component of the signal (plot:3, fig:8.1.5).

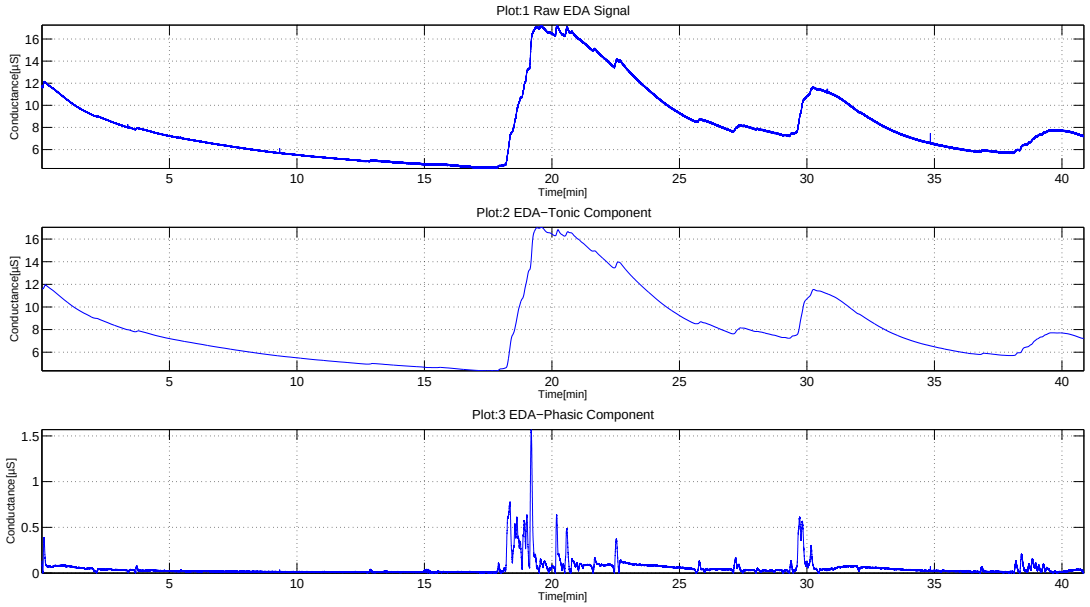

Figure 8.1.5: The tonic and phasic components from the EDA

8.1.4 Respiration Feature Extraction

The features extracted from the respiration signal are the respiration rate and amplitude of respiration (section 4.1.3). The following procedure is adopted for feature extraction:

1. The raw signal is high pass filtered at 0.1 Hz to remove baseline drifting.

2. The resulting waveform is smoothened using a moving window of length 1 second. This signal represents the amplitude of respiration during the test epoch (Plot:2, fig:8.1.6).

3. The respiration rate is extracted using a peak detection algorithm. An absolute threshold for peak detection cannot be defined due to the different baseline values among the subjects arising from varying tautness of the respiration belt when stretched over the diaphragm. The breath intensity also varies among different subjects. Hence we decide a threshold value, so that a local maxima point is identified as a valid peak, only if it is preceded by a value lower than the threshold value (See Plot:2 3, Fig:8.1.6).

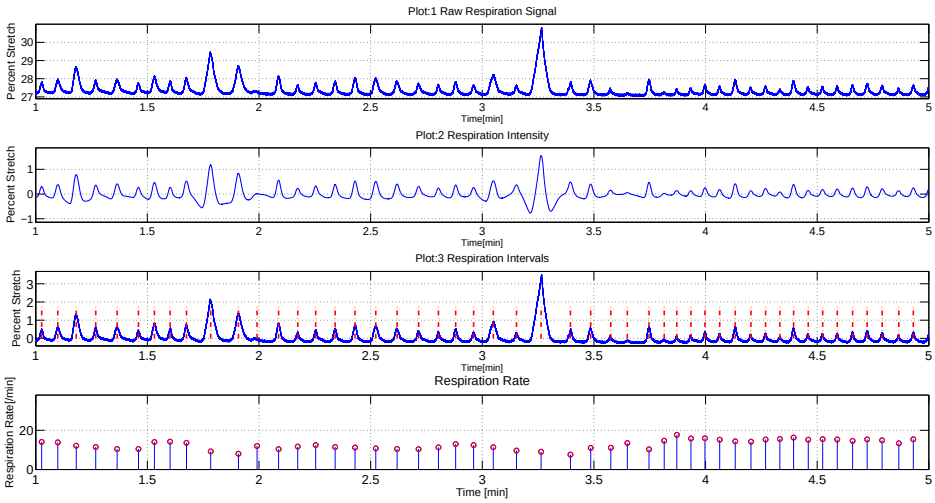

Figure 8.1.6: The features extracted from the respiration signal

8.1.5 EMG Feature Extraction

The feature extracted from the EMG signal is the amplitude of EMG activity. The Root Mean Square of the EMG signal is quasi-linearly related to the force of the respective muscle. The raw signal from the sensor is already RMS averaged and represents the intensity of EMG activity (fig:8.1.7).

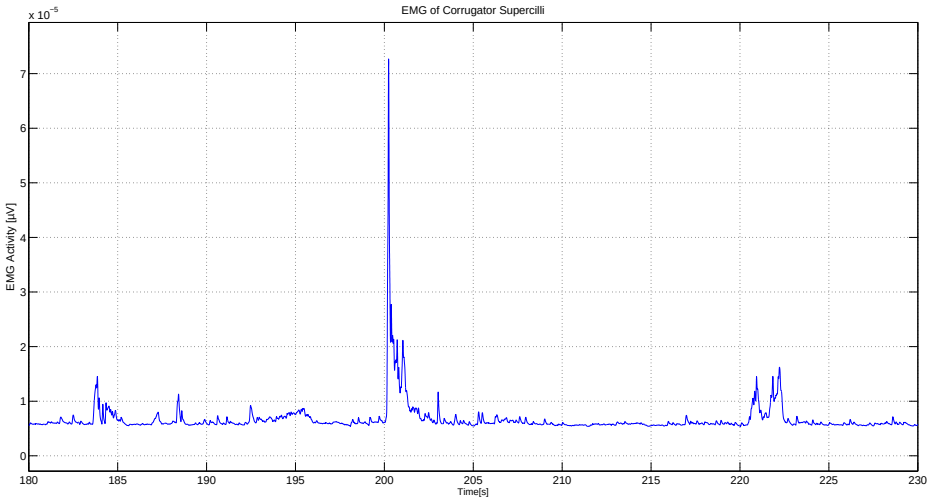

Figure 8.1.7: The EMG of the corrugator supercilli

8.1.6 Data from Labelling System

The raw data acquired from the joystick are distances from the origin on a 2D coordinate graph. These distances are mapped to the equivalent ratings of valence and arousal in the range [0.5 9.5] by normalising them across the geometrical boundary coordinates of the labelling interface

(see section 6.4). The normalisation is done as shown:

$$Valence = 0.5 + 9 \times \frac{(j_x + {}^{x_r}/_2)}{x_r} \tag{8.1}$$

$$Arousal = 0.5 + 9 \times \frac{(j_y + {}^{y_r}/_2)}{y_r} \tag{8.2}$$

where:

j_x is the joystick x coordinate, j_y is the joystick y coordinate, x_r is the range of joystick axis X, y_r is the range of joystick axis Y.

The plot 8.1.8 show the subjective ratings of valence and arousal through the entire video sequence. The blue colored plot denotes the valence and the red colored plot denotes the arousal. These ratings are reduced to affect ratings in Fig.8.1.9.

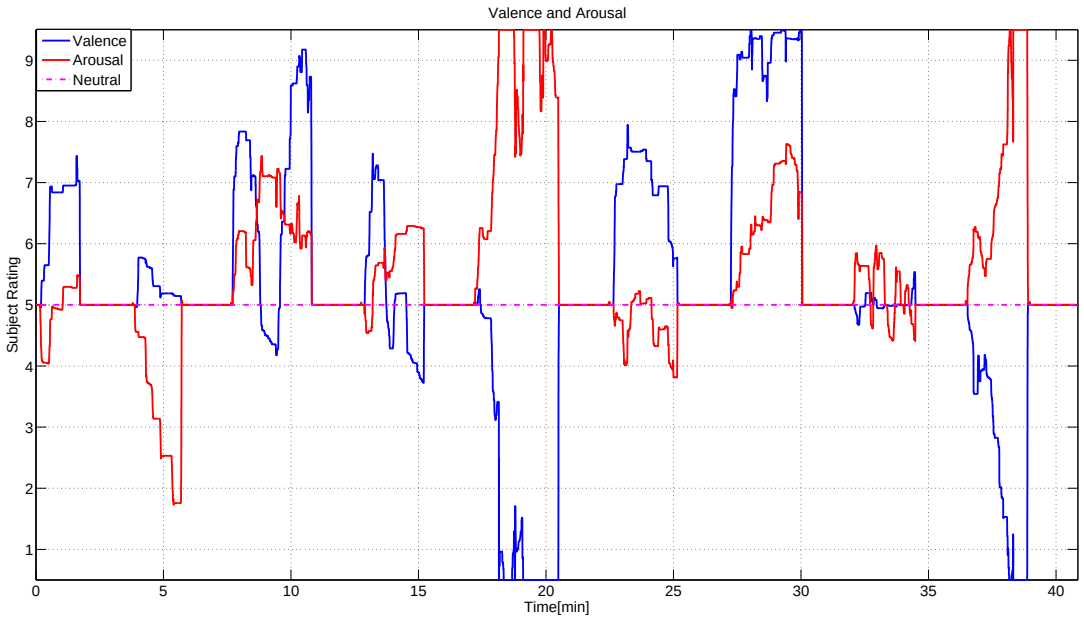

Figure 8.1.8: Subjective ratings of valence and arousal during the entire video sequence

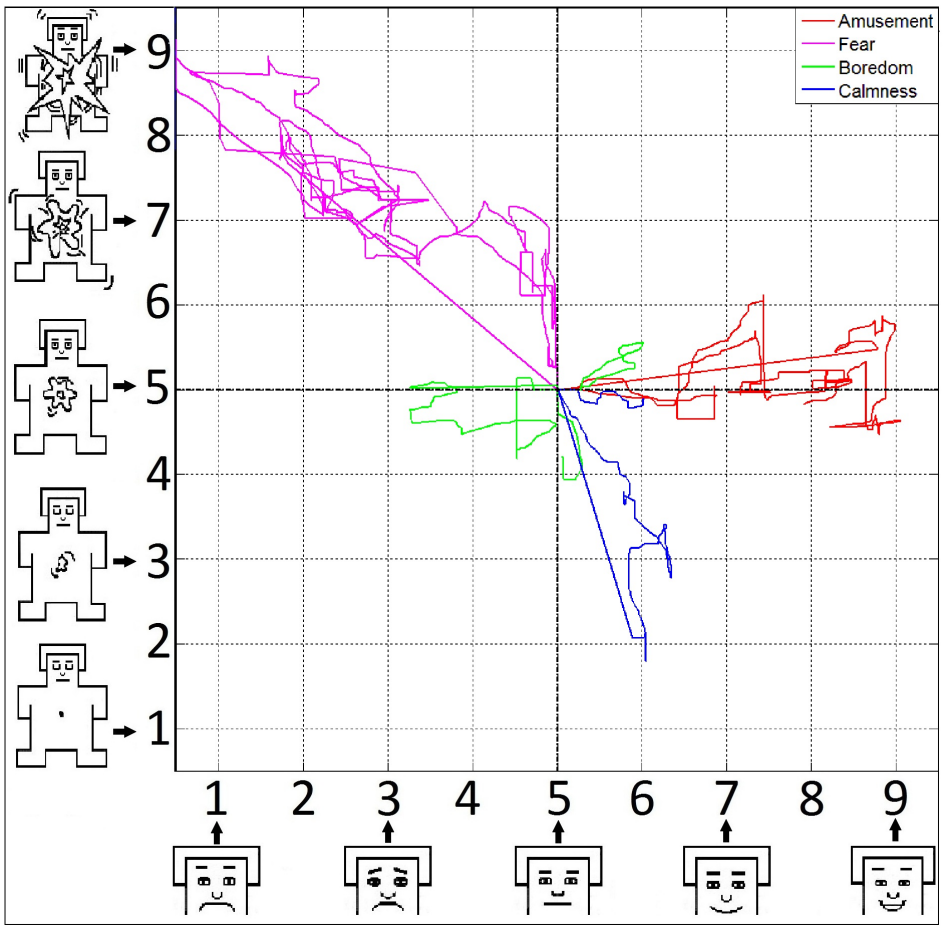

Figure 8.1.9: The reduced subject rating in the valence-arousal space

In this chapter, the extraction of relevant features from the measured biosignals for affect state estimation was discussed. The analysis performed on these features and the results derived thereof are discussed in the last chapter.

Chapter 9

Data Analysis and Results

Affect estimation from biosignals is essentially implemented as a pattern recognition problem. Here the aim is to develop a model that can identify complex patterns from the data set of physiological features and thus recognize the underlying emotions. Various statistical, supervised and unsupervised machine learning techniques are used to analyse the data in affect computing. Van den Broek in [26] has summarized the various classification techniques used in affect estimation studies from 61 scholarly articles.

The primary goal of this thesis being the development and validation of an experiment setup for affect state estimation, a preliminary analysis of data is presented in this chapter. For the same reason only the most fundamental and obvious statistical features are derived from the physiological signals for analysis as discussed. Table 9.1 summarizes the features derived from the physiological signals in the scope of this research work.

Biosignal	Feature extracted
ECG	Heart rate
BVP	Pulse rate
EDA	Intensity of Tonic activity
	Intensity of Phasic activity
Respiration	Respiration rate
	Intensity of Respiration
EMG	Intensity of muscular activity of corrugator supercilli
	Intensity of muscular activity of zygomaticus major

Table 9.1: **Summary of features extracted from the biosignals**

9.1 Feature Space

The following simplifications are applied on the feature data set to reduce computational complexities during the preliminary phase of analysis:

1. **Averaging of features across a video segment-** The features obtained from the physiological signals are averaged across each video segment. Thus for a single subject, each video segment is represented by an 8 dimensional feature vector consisting of mean values of each physiological feature during that video segment. This simplification strips much of the variance from the feature data set and do not reflect the true dynamic nature of the video stimuli responses. However for the preliminary analyses intended here, this simplification is deemed sufficient for a general comprehension of the feature –variations among the different affect classes.

2. **Normalization of features-** To avoid interpersonal differences and to maintain data comparability between different subjects normalization was applied on the features. The following normalization procedure was applied for each subject for each feature[26]:

$$x_n = \frac{x_i - \bar{x}}{\sigma} \tag{9.1}$$

where x_n is the normalized value, x_i the recorded value, $\bar{x}$ the global mean, and σ the standard deviation.

The data sets of all the subjects (30 subjects) are included for analysis after applying the numerical procedures described above. In section 5.2 we introduced the 4 affect classes that are studied in this research work. The subjective evaluations (joystick data) during each affect state (valence and arousal, see section 6.3) are also considered. Thus the data set for analysis is represented by a $30 \times 4 \times 10$ feature vector, where 30 is the number of subjects, 4 are the type of emotion/affect classes and 10 (8 biosignals + 2 joystick data), the number of features derived.

9.2 Features vs. Video Segments

The 10 features (8 physiological features + 2 subjective evaluations of valence and arousal) are compared among the 4 video classes (corresponding to the 4 affect classes under investigation,see section 5.2) to study their variation among the targeted affect expressions (fig:9.2.1).

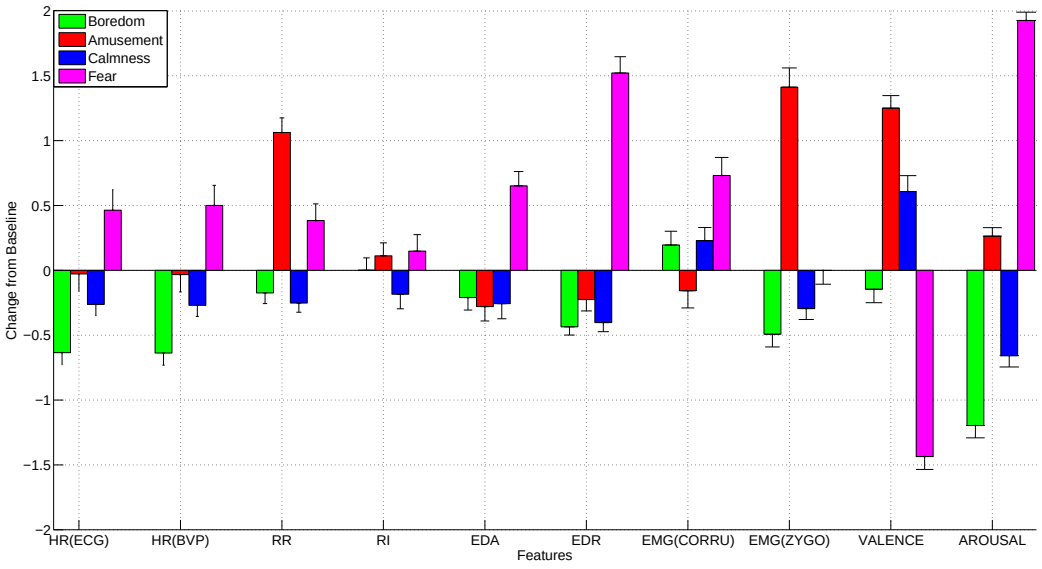

Figure 9.2.1: Means and Standard errors of features for each video class

The means and the standard error of means (SEM) of each features is plotted among the four affect classes. The SEM represents the standard deviation of the feature means and is a measure of how far the feature means are from the true mean of the entire distribution. The SEM is calculated as:

$$SEM = \frac{\sigma}{\sqrt{n}} \tag{9.2}$$

where σ is the standard deviation and n, the no. of samples.

The following conclusions are drawn from the plot 9.2.1:

1. **Cardiac features:**

   (a) **Heart Rate (ECG):** The Heart rate (HR) is the lowest during the video class 'Boredom' and highest for the video class 'Fear'. HR thus clearly varies substantially during negative valence and very high arousal .This is also in agreement with the evidences in literature which associate high heart rate with fear, mental stress etc. (see4.1.1). Higher heart rates are observed during the video segment 'amusement' as compared to the segment 'calmness'. This implies that the subjects were relatively relaxed during the 'calm' video segments.

   (b) **BVP Rate:** The Heart Rate derived from the BVP follows the same pattern as the heart rate derived from the ECG signal. This implies that the ECG and the BVP sensors provide redundant information and for future applications, only one of these

sensors is required. The BVP sensor is preferred over the ECG sensor due to its ease of placement and relative simplicity in data analysis.

2. **Respiration features-** Low respiration rate (RR) with normal intensity of respiration (RI) (i.e, slow, normal breathing) is observed during the 'Boredom' video segments. Comparatively low RR as well as low RI (slow, shallow breathing) is observed during the relaxed states (the 'calmness' video segments). This has been reported by various authors [109], [110], [71] (see 4.1.3). Higher RR and RI are observed during the 'fear' video segments. However the increase in rate and depth of breathing are not well pronounced. This might be due to the fact that not only the intended emotion (anxiety) is elicited during a video stimuli, but other emotions as well which in turn might have an opposite effect [109]. High respiration rates were observed during the 'amusement' video segments, as reported by Boiten et al. [109], where increased RR and RI is associated with excitement and positive affect. The very high respiration rate during this segment might have also arisen from the high-frequency chest movements during laughing [111].

3. **EDA features-** Out of the two features plotted from the EDA activity -the intensity of the EDA signal (EDA) and the intensity of the phasic component of the EDA signal (EDR)-, the latter offers a better discrimination of 'high arousal' from the other classes. Higher EDA intensities are observed during the 'Fear' segment as reported by various authors [112],[113],[68].

4. **EMG features-** The EMG activities of the corrugator supercilli and the zygomaticus major are known differentiators of positive valence from negative valence [74], [75], [76]. This pattern is also observed here -very high corrugator activity during the negative valence ('Fear') segments and high zygomaticus activity during the positive valence ('Amusement') segments. This indicates that the subjects were 'frowning' during the negative affect states and 'laughing/smiling' during the positive affect states.

5. **Subjective evaluation features-** The subjective evaluation features are the valence and the arousal obtained through the labelling interface as explained in 6.3 and 8.1.6. Very high valence and very low arousal are reported for the 'Fear' segment implying that the video stimuli were powerful enough to elicit the targeted affect state of fear. High valence is reported during the 'Amusement' video segments, but the arousal level did not meet the anticipated level. This can be attributed to the familiarity of most of the subjects to one of the 'Amusement' video segments stimuli, which was an excerpt from a recent Hollywood movie. The 'calmness' video segments reported medium levels of valence and arousal was

expected. Finally the 'Boredom' segments achieved expected ratings of low valence and very low arousal.

9.3 Pattern Identification and Visualization

Principal component analysis (PCA) method was applied for pattern identification and visualization of affect states derived from the feature data set. PCA is an unsupervised classification technique that finds structure in the data without known labels. The classification process is based on the similarity of patterns, which is determined by a distance (similarity) measure and an algorithm to generate the clusters of feature vectors representing an emotion state [26]. PCA also reduces the dimensionality of the data while retaining most of the variation in the data set [114]. The PCA algorithm identifies directions called principal components, along which the variation of the data is maximal. The original data is then projected onto these components, preserving as much as variability as possible, there by representing the data in fewer dimensions [115]. This makes possible the visualization of the data in a lower dimensional space and comparison and grouping of data based on spatial distribution (clustering).

9.3.1 Formulation of PCA

PCA is performed on the covariance matrix of the feature data set.

Let

$$X = (x_1, x_2, ...x_n) \tag{9.3}$$

represent the feature data set extracted from the physiological signals, where each x_i is an n dimensional column vector representing the mean value of a feature m for different video segments for all subjects. Let C_x represent the covariance matrix of X, defined as,

$$C_x = cov(x_i, x_j) = \langle (x_i - \mu_i)(x_j - \mu_j) \rangle \tag{9.4}$$

where μ represents the mean of each column vector defined by,

$$\mu = \frac{1}{n} \sum_{i=1}^{n} x_i \tag{9.5}$$

From the covariance matrix, the eigen values and eigenvectors are calculated. The eigenvectors

'ei' and the corresponding eigenvalues '$\lambda i'$ are solutions of the equation:

$$C_x e_i = \lambda_i e_i \tag{9.6}$$

Assuming the λ_i to be distinct, the values of λ_i can be found solving the characteristic equation:

$$| C_x - \lambda I | = 0 \tag{9.7}$$

where I represents the identity matrix.

The eigenvectors representing the principal components are arranged in the order of descending eigenvalues and an ordered orthogonal basis is created with the first eigenvector having the direction of the largest variance of the data [114].

9.3.2 Data Visualisation

From the reduced data set obtained after performing the PCA, the features pertaining to each video segment is color coded and plotted in a 2 dimensional principal component space (figure:9.3.1).

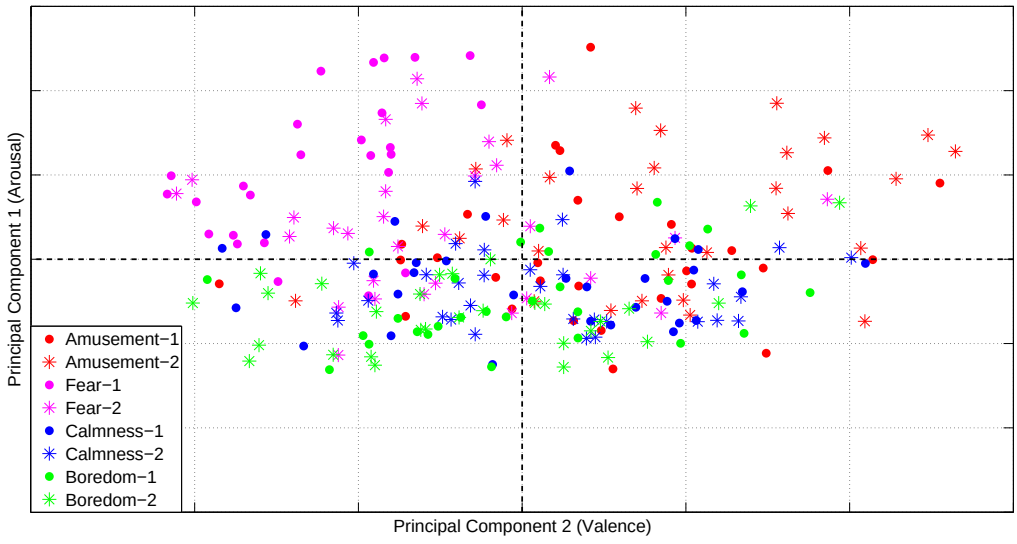

Figure 9.3.1: Visualisation of the 2 principal components of affect Space

The figure 9.3.1 shows the distribution of the feature data set in a 2 dimensional (2D) principal component space. It can be deduced from the figure that the 2D principal components essentially represent the valence and arousal axes of affect space as proposed by [28] (see section 3.1.1), the concept which was used to build the framework of the experiment. The plot also shows clear clustering patterns among the different classes of videos (or the targeted affects)

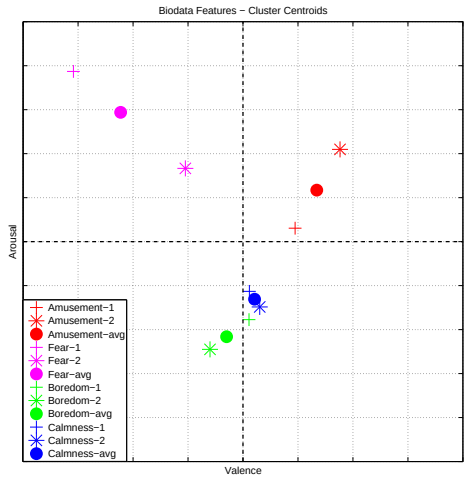

Figure 9.3.2: The cluster centroids from biodata features

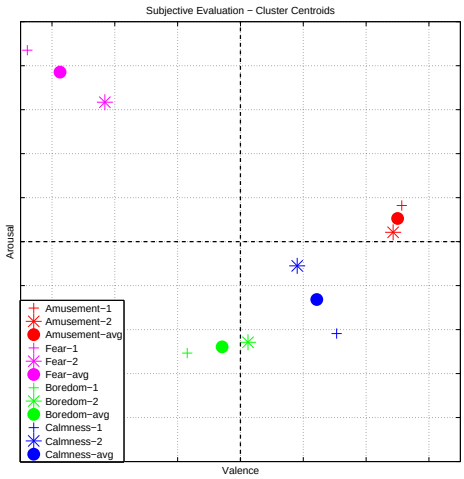

Figure 9.3.3: The cluster centroids from subjective evaluation

as well. The points represented in red color represent videos belonging to quadrant 1 (label-Amusement) in the valence-arousal figure (see fig:5.2.1). Similarly the magenta, green and blue colors represent videos belonging to the 2^{nd} (label-Fear), 3^{rd} (label-Boredom) and 4^{th} (label-Calmness) quadrants respectively. The signs '•' and '*' differentiate between the 2 clips belonging to the same category.

From the reduced feature data set, the centroids of the different clusters were obtained by computing the mean value of coordinate positions of the features tagged by the same color (i.e., pertaining to the same video segment). Similarly centroid positions were also calculated for the clusters of affect, obtained from the subjective evaluation of the affect state through the labelling interface (fig:9.3.2 and 9.3.3). The different color labels distinguish the different affect states as decribed in the previous paragraph. The signs '+' and '*' differentiate between the 2 clips belonging to the same category and the '•' sign represents the cluster centroid of the video segments belonging to the affect category denoted by its color label. Comparing the plots, it can be seen that the affect space described by the bio signals are in unison with the affect space described by the subjective evaluation. This implies that the subjective evaluation of affect states using the labelling interface introduced in this research work is perfectly validated.

9.4 Conclusion and Future work

The development of a framework for the application of affect computing in the context of DLR-RMS has been studied and demonstrated in this research work. An extensive literature review has been conducted on the topic. A labelling system for continuous affect evaluation during dynamic stimuli was developed. Experiments were conducted with 30 subjects and a preliminary

analysis of data was performed. The validity of the proposed concepts were proved from the results obtained.

Further research on the topic include a detailed analysis of the biosignals to identify and derive more features that can shed light into the nature of the affect states that they depict. Instead of representing a video stimulus by a single value of a feature parameter, a continuous evaluation of the feature during the video stimulus can reveal more about the underlying affect states. The same procedure can be applied on the video stimuli that invoked these affect states as well. Here the interesting aspect is the identification of the 'key frames'- frames/points in the video which drive the user to a particular state of affect e.g.,'Fear'. These can be identified by detecting sudden changes in the biosignal features (e.g., sudden Electrodermal response) or by sudden movement of the joystick.

The results derived in this research work also serve as a benchmark for comparison and verification of data, when the framework developed here is adapted into the DLR-RMS.

Appendix A

System Usability Scale (SUS) Survey

Participant ID: _____ Date: ___/___/___

System Usability Scale- Joystick based User Feedback System

Instructions: For each of the following statements, cross one box (with an X) that best describes your opinion about the *joystick based user feedback system* that you used today.

		Strongly Disagree				Strongly Agree
1.	I think that I would like to use this system frequently.	☐	☐	☐	☐	☐
2.	I found the system to be simple.	☐	☐	☐	☐	☐
3.	I thought the system was easy to use.	☐	☐	☐	☐	☐
4.	I think that I could use this system without the support of a technical person.	☐	☐	☐	☐	☐
5.	I found the various functions in this system were well integrated.	☐	☐	☐	☐	☐
6.	I thought there was a lot of consistency in this system.	☐	☐	☐	☐	☐
7.	I would imagine that most people would learn to use this system very quickly.	☐	☐	☐	☐	☐
8.	I found the system very intuitive.	☐	☐	☐	☐	☐
9.	I felt very confident using the system.	☐	☐	☐	☐	☐
10.	I could use the system without having to learn anything new.	☐	☐	☐	☐	☐

Please provide any further comments about this user-feedback system:

This questionnaire is based on the System Usability Scale (SUS), that was developed by John Brooke while working at Digital Equipment Corporation. © Digital Equipment Corporation, 1986. This modified version is based on 'all positive' SUS developed by Jeff Sauro.

Bibliography

[1] J. Hart, A. J. Summerfield, and W. D. Lee, "Motion simulator," June 1988. [Online]. Available: http://www.freepatentsonline.com/4753596.html

[2] Airbus. [Online]. Available: http://www.airbusmilitary.com/Portals/0/Images/Services/PDFs/FULL_FLIGHT_SIMULATOR.pdf

[3] J. Stark, "Motion is there a requirement in large fixed-wing aviation simulators?" 2010.

[4] BMW, "Bmw dynamic driving simulator," August 2013. [Online]. Available: http://www.bmw.tv/web/com/video.do?page=1&videoID=27405&sortType=DISPLAY_DATE&showMyPlaylist=false

[5] Nissan, "Nissan driving simulator," August 2013. [Online]. Available: http://www.nissan-global.com/EN/QUALITY/STORY/SWITCH/

[6] KUKA, "Kuka robocoaster," 2013 June. [Online]. Available: http://www.kuka-entertainment.com/en/products/robocoaster/

[7] V. GT, "Virtualgt simulators," August 2013. [Online]. Available: http://www.virtual-gt.com/

[8] J. Heindl, M. Otter, H. Hirschmller, M. Frommberger, F. Siegert, and H. Heinrich, "The robocoaster simulation platform, path and video generation for an authentic mars flight simulation," 2006.

[9] D. Allerton, "The impact of flight simulation in aerospace," *Aeronautical Journal*, vol. 114, no. 1162, pp. 747–756, 2010.

[10] S. Advani, "The kinematic design of flight simulator motion-bases," Ph.D. dissertation, 1998.

[11] D. Stewart, "A platform with six degrees of freedom," in *Proceedings of the Institution of Mechanical Engineers 1847-1982 (vols 1-196)*, bbbb, Ed., vol. Volume 180 / 1965. Sage Publications, 1965, pp. 371–386.

[12] A. Korobeynikov, V. Turlapov, and N. Novgorod, "Modeling and evaluating of the stewart platform," 2005.

[13] K. Sharma, S. Haddadin, J. Heindl, T. Bellmann, S. Parusel, T. Rokahr, S. Minning, and G. Hirzinger, "Evaluation of human safety in the dlr robotic motion simulator using a crash test dummy," 2013.

[14] T. Bellmann, J. Heindl, M. Hellerer, R. Kuchar, K. Sharma, and G. Hirzinger, "The dlr robot motion simulator part i: Design and setup," in *IEEE International Conference on Robotics and Automation (ICRA)*, may 2011, pp. 4694 –4701.

[15] T. Bellmann, M. Otter, and G. Hirzinger, "The dlr robot motion simulator part ii: Optimization based path-planning," in *IEEE International Conference on Robotics and Automation (ICRA)*, may 2011, pp. 4702 –4709.

[16] T. Bellmann, M. Otter, J. Heindl, and G. Hirzinger, "Real-time path planning for an interactive and industrial robot-based motion simulator," in *Proc. of the 2nd Motion Simulator Conference*, 2007.

[17] K. Sharma, S. Haddadin, J. Heindl, T. Bellmann, S. Parusel, T. Rokahr, S. Minning, and G. Hirzinger, "Serial kinematics based motion simulator - evaluation of safety of the passenger," 2013.

[18] "Motion perception and simulation," April 2014. [Online]. Available: http://www.kyb.tuebingen.mpg.de/?id=526

[19] A. Roscoe, "Assessing pilot workload. why measure heart rate, hrv and respiration?" *Biological psychology*, vol. 34, no. 2, pp. 259–287, 1992.

[20] J. A. Caldwell, "Fatigue in aviation," *Travel Medicine and Infectious Disease*, vol. 3, no. 2, pp. 85–96, 2005.

[21] R. BOWLES and A. POPE, "A program for assessing pilot mental state in flight simulators," no. t, 1982.

[22] J. B. Brookings, G. F. Wilson, and C. R. Swain, "Psychophysiological responses to changes in workload during simulated air traffic control," *Biological psychology*, vol. 42, no. 3, pp. 361–377, 1996.

[23] J. Veltman and A. Gaillard, "Physiological indices of workload in a simulated flight task," *Biological psychology*, vol. 42, no. 3, pp. 323–342, 1996.

[24] B. O. Rothbaum, L. Hodges, B. A. Watson, G. D. Kessler, and D. Opdyke, "Virtual reality exposure therapy in the treatment of fear of flying: A case report," *Behaviour Research and Therapy*, vol. 34, no. 5, pp. 477–481, 1996.

[25] A. Muhlberger, G. Wiedemann, and P. Pauli, "Efficacy of a one-session virtual reality exposure treatment for fear of flying," *Psychotherapy Research*, vol. 13, no. 3, pp. 323–336, 2003.

[26] E. L. van den Broek, "Affective signal processing (asp): Unraveling the mystery of emotions," Ph.D. dissertation, University of Twente, Enschede, September 2011.

[27] J. Kleinginna, P. R, and A. M. Kleinginna, "A categorized list of emotion definitions, with suggestions for a consensual definition," *Motivation and emotion*, vol. 5, no. 4, pp. 345–379, 1981.

[28] J. A. Russell, "Core affect and the psychological construction of emotion." *Psychological review*, vol. 110, no. 1, p. 145, 2003.

[29] R. E. Thayer, *The biopsychology of mood and arousal.* Oxford University Press, 1989.

[30] D. Watson and A. Tellegen, "Toward a consensual structure of mood." *Psychological bulletin*, vol. 98, no. 2, p. 219, 1985.

[31] N. Morris, William and P. Schnurr, Paula, *Mood: The frame of mind.* Springer-Verlag Publishing, 1989.

[32] P. J. Lang, "The emotion probe: Studies of motivation and attention." *American psychologist*, vol. 50, no. 5, p. 372, 1995.

[33] "Functions of autonomic nervous system," April 2014. [Online]. Available: http://www.medtronicrdn.com/

[34] R. Picard, "Picard, affective computing," August 2013. [Online]. Available: http://www.youtube.com/watch?v=ujxriwApPP4

[35] P. Rani, N. Sarkar, C. Smith, and L. Kirby, "Anxiety detecting robotic system- towards implicit humanrobot collaboration," *Robotica*, vol. 22, pp. 85–95, 2004.

[36] S. D. Kreibig, "Autonomic nervous system activity in emotion: A review," *Biological psychology*, vol. 84, no. 3, pp. 394–421, 2010.

[37] C. Collet, E. Vernet-Maury, G. Delhomme, and A. Dittmar, "Autonomic nervous system response patterns specificity to basic emotions," *Journal of the autonomic nervous system*, vol. 62, no. 1-2, pp. 45–57, 1997.

[38] P. Ekman, R. W. Levenson, and W. V. Friesen, "Autonomic nervous system activity distinguishes among emotions," *Science*, vol. 221, no. 4616, pp. 1208–1210, 1983.

[39] R. Picard, "Affective computing," M.I.T Media Laboratory Perceptual Computing Section, Tech. Rep., 1995.

[40] R. W. Picard, E. Vyzas, and J. Healey, "Toward machine emotional intelligence: Analysis of affective physiological state," *Pattern Analysis and Machine Intelligence, IEEE Transactions on*, vol. 23, no. 10, pp. 1175–1191, 2001.

[41] J. A. Healey, "Wearable and automotive systems for affect recognition from physiology," Ph.D. dissertation, Massachusetts Institute of Technology, 2000.

[42] P. Rani, N. Sarkar, C. A. Smith, and J. A. Adams, "Affective communication for implicit human-machine interaction," in *Systems, Man and Cybernetics, 2003. IEEE International Conference on*, vol. 5. IEEE, 2003, pp. 4896–4903.

[43] C. Liu, P. Rani, and N. Sarkar, "Human-robot interaction using affective cues," in *Robot and Human Interactive Communication, 2006. ROMAN 2006. The 15th IEEE International Symposium on.* IEEE, 2006, pp. 285–290.

[44] C. D. Spielberger, *State-Trait Anxiety Inventory.* John Wiley & Sons, Inc., 2010. [Online]. Available: http://dx.doi.org/10.1002/9780470479216.corpsy0943

[45] P. Rani, C. Liu, N. Sarkar, and E. Vanman, "An empirical study of machine learning techniques for affect recognition in human–robot interaction," *Pattern Analysis and Applications*, vol. 9, no. 1, pp. 58–69, 2006.

[46] D. Kulic and E. Croft, "Estimating robot induced affective state using hidden markov models," in *The 15th IEEE International Symposium on Robot and Human Interactive Communication*, 2006.

[47] katsis, katertsidis, ganiatsas, and fotiadis, "Toward emotion recognition in car-racing drivers - a biosignal processing approach," 2008.

[48] C. Liu, K. Conn, N. Sarkar, and W. Stone, "Affect recognition in robot assisted rehabilitation of children with autism spectrum disorder," in *Robotics and Automation, 2007 IEEE International Conference on.* IEEE, 2007, pp. 1755–1760.

[49] K. H. Kim, S. W. Bang, and S. R. Kim, "Emotion recognition system using short-term monitoring of physiological signals," 2004.

[50] Hudlicka and Mcneese, "Assessment of user affective and belief states for interface adaptation - application to air force pilot task -," 2002.

[51] J. Zhai and A. Barreto, "Stress recognition using non-invasive technology," 2006.

[52] J. Scheirer, R. Fernandez, J. Klein, and R. W. Picard, "Frustrating the user on purpose: a step toward building an affective computer," *Interacting with computers*, vol. 14, no. 2, pp. 93–118, 2002.

[53] H. Prendinger, J. Mori, and M. Ishizuka, "Using human physiology to evaluate subtle expressivity of a virtual quizmaster in a mathematical game," *International journal of human-computer studies*, vol. 62, no. 2, pp. 231–245, 2005.

[54] C. Lisetti and F. Nasoz, "Using noninvasive wearable computers to recognize human emotions from physiological signals," *EURASIP Journal on Applied Signal Processing*, vol. 2004, pp. 1672–1687, 2004.

[55] E. L. Van Den Broek, M. H. Schut, J. H. Westerink, J. van Herk, and K. Tuinenbreijer, "b," in *Computer Vision in Human-Computer Interaction*. Springer, 2006, pp. 52–63.

[56] H. Gunes, M. Piccardi, and M. Pantic, "From the lab to the real world: Affect recognition using multiple cues and modalities," 2008.

[57] R. W. Levenson, "Autonomic nervous system differences among emotions," *Psychological science*, vol. 3, no. 1, pp. 23–27, 1992.

[58] M. Mulder, M. R. van Paassen, and E. R. Boer, "Exploring the roles of information in the manual control of vehicular locomotion: From kinematics and dynamics to cybernetics," *Presence: Teleoperators and Virtual Environments*, vol. 13, no. 5, pp. 535–548, 2004.

[59] medical dictionary.com, "Electrocardiogram," April 2014. [Online]. Available: http: \medical-dictionary.thefreedictionary.com+complexes

[60] O. Rompelman, A. Coenen, and R. Kitney, "Measurement of heart-rate variability: Part 1comparative study of heart-rate variability analysis methods," *Medical and Biological Engineering and Computing*, vol. 15, no. 3, pp. 233–239, 1977.

[61] B. M. Appelhans and L. J. Luecken, "Heart rate variability as an index of regulated emotional responding," *Review of General Psychology*, vol. 10, no. 3, pp. 229–240, 2006.

[62] R. B. Northrop, *Noninvasive instrumentation and measurement in medical diagnosis*. CRC Press, 2001.

[63] W. Karlen, K. Kobayashi, J. Ansermino, and G. Dumont, "Photoplethysmogram signal quality estimation using repeated gaussian filters and cross-correlation," *Physiological measurement*, vol. 33, no. 10, p. 1617, 2012.

[64] J. Allen, "Photoplethysmography and its application in clinical physiological measurement," *Physiological measurement*, vol. 28, no. 3, p. R1, 2007.

[65] M. J. Christie, "Electrodermal activity in the 1980s: a review." *Journal of the Royal Society of Medicine*, vol. 74, no. 8, p. 616, 1981.

[66] C. Collet, F. Di Rienzo, N. El Hoyek, and A. Guillot, "Autonomic nervous system correlates in movement observation and motor imagery," *Frontiers in human neuroscience*, vol. 7, 2013.

[67] W. Boucsein, *Electrodermal activity*. Springer, 2012, vol. ttt.

[68] M. E. Dawson, A. M. Schell, and D. L. Filion, "The electrodermal system," *Handbook of psychophysiology*, p. 159, 2007.

[69] R. S. Woodworth and H. Schlosberg, *Experimental psychology*. Oxford and IBH Publishing, 1954.

[70] L. Haward, "Assessment of stress-tolerance in commercial pilots." *Flight Safety*, 1967.

[71] C. J. Wientjes, "Respiration in psychophysiology: methods and applications," *Biological Psychology*, vol. 34, no. 2, pp. 179–203, 1992.

[72] S. S. Tomkins, "Affect theory," *Approaches to emotion*, vol. 163, no. b, p. 195, 1984.

[73] U. Dimberg, M. Thunberg, and K. Elmehed, "Unconscious facial reactions to emotional facial expressions," *Psychological science*, vol. 11, no. 1, pp. 86–89, 2000.

[74] P. J. Lang, M. M. Bradley, and B. N. Cuthbert, "Emotion, motivation, and anxiety: brain mechanisms and psychophysiology," *Biological psychiatry*, vol. 44, no. 12, pp. 1248–1263, 1998.

[75] A. J. Fridlund and J. T. Cacioppo, "Guidelines for human electromyographic research," *Psychophysiology*, vol. 23, no. 5, pp. 567–589, 1986.

[76] L. H. Epstein, "Perception of activity in the zygomaticus major and corrugator supercilii muscle regions," *Psychophysiology*, vol. 27, no. 1, pp. 68–72, 1990.

[77] R. W. Levenson, L. L. Carstensen, W. V. Friesen, and P. Ekman, "Emotion, physiology, and expression in old age." *Psychology and aging*, vol. 6, no. 1, p. 28, 1991.

[78] P. Vos, P. De Cock, V. Munde, K. Petry, W. Van Den Noortgate, and B. Maes, "The tell-tale: What do heart rate; skin temperature and skin conductance reveal about emotions of people with severe and profound intellectual disabilities?" *Research in developmental disabilities*, vol. 33, no. 4, pp. 1117–1127, 2012.

[79] J. A. Russell, "A circumplex model of affect," *Journal of Personality and Social Psychology*, vol. 39, pp. 1161–1178, 1980.

[80] "Thrill, cambridge dictionaries, n.d. web. 4 apr. 2014," April 2014. [Online]. Available: http://dictionary.cambridge.org/dictionary/british/thrill_1?q=thrill

[81] "Fear,cambridge dictionaries, n.d. web. 4 apr. 2014." April 2014. [Online]. Available: http://dictionary.cambridge.org/dictionary/british/fear_1?q=Fear

[82] "Boredom, merriam-webster.com. merriam-webster, n.d. web. 4 apr. 2014." April 2014. [Online]. Available: http://www.merriam-webster.com/dictionary/boredom

[83] "Calmness, macmillan dictionary, n.d. web. 4 apr. 2014." April 2014. [Online]. Available: http://www.macmillandictionary.com/dictionary/british/calm#calmness

[84] J. J. Gross and R. W. Levenson, "Emotion elicitation using films," *Cognition & Emotion*, vol. 9, no. 1, pp. 87–108, 1995.

[85] J. Hewig, D. Hagemann, J. Seifert, M. Gollwitzer, E. Naumann, and D. Bartussek, "Brief report," *Cognition & Emotion*, vol. 19, no. 7, pp. 1095–1109, 2005.

[86] P. Philippot, "Inducing and assessing differentiated emotion-feeling states in the laboratoryr," *Cognition & Emotion*, vol. 7, no. 2, pp. 171–193, 1993.

[87] D. L. Fisher, M. Rizzo, J. Caird, and J. D. Lee, *Handbook of driving simulation for engineering, medicine, and psychology.* CRC Press, 2011.

[88] J. Rottenberg, R. D. Ray, and J. J. Gross, "Emotion elicitation using films." 2007.

[89] M. Soleymani, J. Davis, and T. Pun, "A collaborative personalized affective video retrieval system," in *Affective Computing and Intelligent Interaction and Workshops, 2009. ACII 2009. 3rd International Conference on.* IEEE, 2009, pp. 1–2.

[90] R. W. Levenson, "Emotion and the autonomic nervous system: A prospectus for research on autonomic specificity," *Social psychophysiology and emotion: Theory and clinical applications*, pp. 17–42, 1988.

[91] J. Sauro, *A practical guide to the System Usability Scale (SUS): Background, benchmarks & best practices*. Denver,CO: Measuring Usability LLC., 2011.

[92] A. Bangor, P. Kortum, and J. Miller, "Determining what individual sus scores mean: Adding an adjective rating scale," *Journal of usability studies*, vol. 4, no. 3, pp. 114–123, 2009.

[93] M. M. Bradley and P. J. Lang, "Measuring emotion: the self-assessment manikin and the semantic differential," *Journal of behavior therapy and experimental psychiatry*, vol. 25, no. 1, pp. 49–59, 1994.

[94] T. T. Ltd., April 2014. [Online]. Available: http://www.thoughttechnology.com/sensors.htm

[95] N. Instruments, "Ni-9205," April 2014. [Online]. Available: http://sine.ni.com/nips/cds/view/p/lang/de/nid/208800

[96] ——, "Labview 2013," April 2014. [Online]. Available: http://www.ni.com/labview/d/

[97] "Ecg sensor," April 2014. [Online]. Available: http://thoughttechnology.com/sciencedivision/pages/products/ekg.html

[98] W. B. Mendes, "Assessing autonomic nervous system activity," *Methods in social neuroscience*, pp. 118–147, 2009.

[99] F. Shaffer and D. C. Combatalade, "Don't add or miss a beat: A guide to cleaner heart rate variability recordings," *Biofeedback*, vol. 41, no. 3, pp. 121–130, 2013.

[100] R. Piacentini, "Emotions at fingertips, revealing individual features in galvanic skin response signals," Ph.D. dissertation, Universitgli studi di Roma La Sapienza,Rome, 2004.

[101] April 2014. [Online]. Available: http://thoughttechnology.com/sciencedivision/media/books/MAR908-03%20SEMG%20applied%20to%20physical%20rehabilitation%20and%20biomechanics.pdf

[102] "Matlab," April 2014. [Online]. Available: http://www.mathworks.de/products/matlab/

[103] P. S. Hamilton and W. J. Tompkins, "Quantitative investigation of qrs detection rules using the mit/bih arrhythmia database," *Biomedical Engineering, IEEE Transactions on*, no. 12, pp. 1157–1165, 1986.

[104] H. Sedghamiz, "Complete pan tompkins implementation ecg qrs detector," April 2014. [Online]. Available: http://www.mathworks.com/matlabcentral/fileexchange/45840-complete-pan-tompkins-implementation-ecg-qrs-detector

[105] P. Rani and N. Sarkar, "Emotion-sensitive robots-a new paradigm for human-robot interaction," in *Humanoid Robots, 2004 4th IEEE/RAS International Conference on*, vol. 1. IEEE, 2004, pp. 149–167.

[106] J. Pan and W. J. Tompkins, "A real-time qrs detection algorithm," *Biomedical Engineering, IEEE Transactions on*, no. 3, pp. 230–236, 1985.

[107] A. Johansson, P. Å. Öberg, and G. Sedin, "Monitoring of heart and respiratory rates in newborn infants using a new photoplethysmographic technique," *Journal of clinical monitoring and computing*, vol. 15, no. 7-8, pp. 461–467, 1999.

[108] C. Yu, Z. Liu, T. McKenna, A. T. Reisner, and J. Reifman, "A method for automatic identification of reliable heart rates calculated from ecg and ppg waveforms," *Journal of the American Medical Informatics Association*, vol. 13, no. 3, pp. 309–320, 2006.

[109] F. A. Boiten, N. H. Frijda, and C. J. Wientjes, "Emotions and respiratory patterns: review and critical analysis," *International Journal of Psychophysiology*, vol. 17, no. 2, pp. 103–128, 1994.

[110] E. B. Skaggs, "Studies in attention and emotion." *Journal of Comparative Psychology*, vol. 10, no. 4, p. 375, 1930.

[111] S. Svebak, "Respiratory patterns as predictors of laughter," *Psychophysiology*, vol. 12, no. 1, pp. 62–65, 1975.

[112] F. Esteves, U. Dimberg, and A. Öhman, "Automatically elicited fear: Conditioned skin conductance responses to masked facial expressions," *Cognition & Emotion*, vol. 8, no. 5, pp. 393–413, 1994.

[113] S. D. Kreibig, F. H. Wilhelm, W. T. Roth, and J. J. Gross, "Cardiovascular, electrodermal, and respiratory response patterns to fear-and sadness-inducing films," *Psychophysiology*, vol. 44, no. 5, pp. 787–806, 2007.

[114] I. Jolliffe, *Principal component analysis*. Wiley Online Library, 2005.

[115] M. Ringner, "What is principal component analysis?" *Nature biotechnology*, vol. 26, no. 3, pp. 303–304, 2008.

List of Figures

1.2.1 Modern motion-flight simulator based on Stewart Platform 18
1.3.1 The DLR Robotic Motion Simulator (DLR-RMS) 19
1.4.1 Simulator perception space 20

3.1.1 Valence-Arousal model of emotion 26
3.1.2 Functions of ANS 27
3.2.1 Human-machine interface based on affect states, proposed by Rani et al. 29

4.1.1 Schematic diagram of normal sinus rhythm for human heart 32
4.1.2 An example of a heart rate variability power spectrum 33
4.1.3 The BVP signal 33
4.1.4 The typical EDA signal 34
4.1.5 The respiration signal 35
4.1.6 A typical facial EMG signal (RMS valued) 36

5.2.1 The Valence-Arousal model (VA) by Russell. 42
5.3.1 The structue of the proposed experiment 44

6.4.1 The joystick interface system 47
6.4.2 The user interface 49
6.4.3 The video with the user interface display 49
6.5.1 The instrumentation architecture developed for affect estimation 50
6.6.1 The state Machine architecture developed for the experiment 51
6.6.2 The joystick interface initialisation and the DAQ initialisation implemented in LabVIEW 52
6.6.3 The data acquisition state implemented in LabVIEW 53

7.3.1 The ECG electrode position 56
7.3.2 The BVP sensor position 57
7.3.3 The skin conductance sensor position 58

7.3.4 The respiration sensor position 58
7.3.5 The temperature sensor position 59
7.3.6 The EMG sensor position 60
7.4.1 The sensors attached on the test subject 60

8.1.1 Interbeat intervals from the ECG signal 67
8.1.2 Heart rate extracted from the ECG signal 68
8.1.3 Interbeat intervals from BVP signal 68
8.1.4 Heart rate from BVP signal 69
8.1.5 The tonic and phasic components from the EDA 70
8.1.6 The features extracted from the respiration signal 71
8.1.7 The EMG of the corrugator supercilli 71
8.1.8 Subjective ratings of valence and arousal during the entire video sequence 72
8.1.9 The reduced subject rating in the valence-arousal space 73

9.2.1 Means and Standard errors of features for each video class 77
9.3.1 Visualisation of the 2 principal components of affect Space 80
9.3.2 The cluster centroids from biodata features 81
9.3.3 The cluster centroids from subjective evaluation 81

List of Tables

5.1 **The meanings of the intended affect states in a dictionary.** 43

6.1 **The video stimuli set.** 46

8.1 **Summary of the features derived from biosignals.** 66

9.1 **Summary of features extracted from the biosignals** 75